SMAI-JCM
SMAI Journal of Computational Mathematics

A BD-entropy inequality preserving Finite Volume scheme for the Quantum Navier–Stokes system

Caterina Calgaro, Robin Colombier & Emmanuel Creusé

Volume 12 (2026), p. 43-73.
https://doi.org/10.5802/jcm.143

The SMAI Journal of Computational Mathematics is a member of the Centre Mersenne for Open Scientific Publishing
http://www.centre-mersenne.org/
Submissions at https://smai-jcm.centre-mersenne.org/ojs/submission
e-ISSN: 2426-8399

SMAI Journal of Computational Mathematics
Vol. 12, 43-73 (2026)

A BD-entropy inequality preserving Finite Volume scheme for the Quantum Navier–Stokes system

Caterina Calgaro [1]
Robin Colombier [2]
Emmanuel Creusé [3]

[1] Université de Lille, Laboratoire Paul Painlevé UMR 8524, 59665 Villeneuve d'Ascq Cedex, France
E-mail address: caterina.calgaro@univ-lille.fr
[2] Université Polytechnique Hauts-de-France, INSA Hauts-de-France, CERAMATHS, 59313 Valenciennes, France
E-mail address: robin.colombier@uphf.fr
[3] Université Polytechnique Hauts-de-France, INSA Hauts-de-France, CERAMATHS, 59313 Valenciennes, France
E-mail address: emmanuel.creuse@uphf.fr.

Abstract. In this work, we propose a Finite-Volume scheme on cartesian grids for the numerical approximation of some solutions of the Quantum Navier–Stokes (QNS) equations. An augmented formulation is implemented by introducing an additional drift velocity $\mathbf{v}$, which reduces the third-order quantum operator to a second-order operator. A set of QNS equations is thus obtained for the density ρ, the drift velocity $\mathbf{v} = \nabla \log \rho$ and the so-called effective velocity $\mathbf{w} = \mathbf{u} + \nu\mathbf{v}$, where $\mathbf{u}$ is the fluid velocity and ν its kinematic viscosity. This formulation includes both the case $\nu = 0$ (Quantum Euler equations) and $\nu > 0$. The originality of our contribution lies in proposing a scheme that provides some discrete BD-entropy inequalities, similarly to the continuous case, for the system in $(\rho, \mathbf{w}, \mathbf{v})$. To do this, we consider a numerical scheme based on a time splitting strategy. The first step consists of a classical first-order Finite-Volume scheme for the hyperbolic part. The second step includes second order terms and source terms, some of which must be carefully discretized. This step is treated implicitly but only requires the inversion of a linear system. Discrete BD-entropy inequalities are established in dimension d. Moreover, for $d = 1$, this result is extended to so-called κ-entropies. Numerical tests in one and two dimensions illustrate the efficiency of the scheme in several configurations.

2020 Mathematics Subject Classification. 35Q30, 35Q40, 65M08.
Keywords. Quantum Navier–Stokes equations, Finite Volume method, BD-entropy inequality.

1. Introduction

The Quantum Navier–Stokes (QNS) system corresponds to a generalization of the usual Navier–Stokes system when quantum effects need to be taken into account, as in certain physical phenomena such as superfluids evolution, electron flow in semiconductors or Bose–Einstein condensates. It can be shown that the QNS system corresponds to a limit hydrodynamic model derived from the kinetic description of a fluid by the Wigner–Fokker–Planck equation, associated with a Chapman–Enskog expansion [9]. In fact, the QNS system is nothing other than the usual Navier–Stokes system, to which a third-order quantum correction term is added in the momentum equation, called the "Bohm potential", see the system (1.1) below. Note that the QNS system can also be considered as a particular case of the general Navier–Stokes Korteweg (NSK) system derived from multiphase flow modelling, see [8] and

C. Calgaro acknowledges the support of the CDP C2EMPI, as well as the French State under the France-2030 programme, the University of Lille, the Initiative of Excellence of the University of Lille, the European Metropolis of Lille for their funding and support of the R-CDP-24-004-C2EMPI project.
https://doi.org/10.5802/jcm.143

references therein, where the capillarity coefficient and the shear and apparent viscosities are given by particular functions.

From the continuous point of view, some recent contributions have derived theoretical results on the QNS and NSK models. For example, the global existence of weak solutions has been established in [20] for the QNS system in the case of a linear dependent viscosity. In [27] the authors construct global weak solutions to the QNS system and perform the semi-classical limit to the associated compressible NS equations. The aim in [7] is to show that a global weak solution of the QNS system (which is also a dissipative solution) converges to a dissipative solution of the quantum Euler system. In [8] the exponential decay of the solution towards a stationary state has been studied for the NSK system with a drag term. In all these papers, the starting point is a so-called Bresch–Desjardins (BD) entropy inequality (see Proposition 10 in [20], Introduction and Appendix A in [27], Propositions 3 and 4 in [7] and the assumptions of Definition 2 in [8]), initially coming from a seminal work from Bresch and Desjardins [4, 5]. In order to establish the BD-entropy inequalities, the authors introduce a new variable $\mathbf{w}$ corresponding to the so-called "effective velocity", defined as $\mathbf{w} = \mathbf{u} + \nu\nabla\log\rho$, where $\mathbf{u}$ is the fluid velocity, ν its kinematic viscosity and ρ its density. Note that such BD-entropy inequalities are also needed in other contexts, such as the study of the existence of certain solutions of the compressible NS system with degenerate viscosities, see Remark 2 in [6] where an estimate of κ-entropy is provided. For a recent survey of the vast bibliography devoted to global existence results for the NSK and QNS systems, we refer in particular to the introduction in [8].

In this paper, we focus on the numerical aspects of approximating the solutions of the QNS system. The main difficulty lies in the presence of the Bohm potential in the momentum equation, which corresponds to a third-order term, increasing the complexity of the numerical scheme used to obtain approximate solutions. Several methods have been proposed in the literature for NSK and/or QNS systems. One possibility is to discretize the original system directly. In this case, we can cite, for example, the use of $H^2(\Omega)$-conform elements associated with a variational formulation for approximating the isothermal NSK system [21], the use of some $\mathcal{C}^1 - B$ splines associated with a least squares method for calculating multiphase flows using the NSK equations [29], or a finite difference method in a 1D stationary case of the QNS system [24]. A second way of proceeding is to introduce several additional unknowns, in order to obtain an augmented system of first order only, allowing the use of standard classical finite volume or discontinuous Galerkin methods. In this case, we can cite, for example, the reformulation of the defocused nonlinear Schrödinger equation [10, 13], the approximation of the NSK equations for modeling the dynamics of a compressible fluid [11, 12, 15, 32] or the thin films flow simulation subject to capillarity and viscosity [14]. A third possibility is to introduce a new variable $\mathbf{v} = \nabla f(\rho)/\rho$ where the function f must be specified and to add to the original third-order system an additional equation, allowing it to be reduced to a second-order one. Examples include the surface tension approximation of the shallow water system [2], the Euler–Korteweg equations [3], the NSK system using a relaxation technique [23, 26, 30], or the surface tension modeling including the full curvatuves of the free surface [31]. In this work, we focus on this third possibility for the QNS system. The barotropic Quantum Navier–Stokes equations reads for $t \in]0, T]$ and $\mathbf{x} \in \Omega$ as:

$$\partial_t\rho + \operatorname{div}(\rho\mathbf{u}) = 0, \tag{1.1a}$$

$$\partial_t(\rho\mathbf{u}) + \operatorname{div}(\rho\mathbf{u}\otimes\mathbf{u}) + \nabla p(\rho) - 2\varepsilon^2\rho\nabla\left(\frac{\Delta\sqrt{\rho}}{\sqrt{\rho}}\right) + r\rho\mathbf{u} = 2\nu\operatorname{div}(\rho D(\mathbf{u})), \tag{1.1b}$$

$$\rho_{|t=0} = \rho_0, \qquad (\rho\mathbf{u})_{|t=0} = \rho_0\mathbf{u}_0. \tag{1.1c}$$

Here, $T > 0$, $\Omega = \mathbb{T}^d$ is the torus in dimension d ($1 \le d \le 3$), and $\mathbf{u}\otimes\mathbf{u}$ the matrix with components u_iu_j. The function $p(\rho) = \rho^\gamma$ with $\gamma > 1$ is the pressure, and $D(\mathbf{u})$ stands for the symmetric part of the velocity gradient, namely $D(\mathbf{u}) = (\nabla\mathbf{u} + \nabla^T\mathbf{u})/2$. Finally, the physical parameters are the reduced Planck constant $\varepsilon > 0$, the viscosity constant $\nu > 0$ and the drag coefficient $r > 0$.

We introduce the energy $\mathcal{E}_\varepsilon$ of the system corresponding to the sum of the kinetic, quantum and internal energies as:

$$\mathcal{E}_\varepsilon(\rho,\mathbf{u}) = \int_\Omega \frac{\rho}{2}\Big(|\mathbf{u}|^2 + \varepsilon^2|\nabla\log\rho|^2\Big) + \frac{\rho^\gamma}{\gamma-1}\mathrm{d}\mathbf{x}. \tag{1.2}$$

Using a formal computation, we easily obtain:

$$\frac{\mathrm{d}\mathcal{E}_\varepsilon}{\mathrm{d}t}(\rho,\mathbf{u}) + \nu\int_\Omega \rho|D(\mathbf{u})|^2\mathrm{d}\mathbf{x} + r\int_\Omega \rho|\mathbf{u}|^2\mathrm{d}\mathbf{x} = 0. \tag{1.3}$$

In addition to the energy estimate (1.3), a BD-entropy equality can be proved. Introducing

$$\mathbf{v} = \nabla\log\rho, \quad \text{the drift velocity,} \tag{1.4}$$

$$\mathbf{w} = \mathbf{u} + \nu\mathbf{v}, \quad \text{the effective velocity,} \tag{1.5}$$

and defining the BD-Entropy E_ε by :

$$E_\varepsilon(\rho,\mathbf{v},\mathbf{w}) = \int_\Omega e_\varepsilon(\rho,\mathbf{v},\mathbf{w})\mathrm{d}\mathbf{x} \tag{1.6}$$

where

$$e_\varepsilon(\rho,\mathbf{v},\mathbf{w}) = \frac{\rho}{2}\Big(|\mathbf{w}|^2 + (\varepsilon^2+\nu^2)|\mathbf{v}|^2\Big) + \frac{\rho^\gamma}{\gamma-1} + r\nu\rho\log\rho, \tag{1.7}$$

it can be proved that

$$\frac{\mathrm{d}E_\varepsilon}{\mathrm{d}t}(\rho,\mathbf{v},\mathbf{w}) + \nu\Big[\int_\Omega \gamma\rho^{\gamma-2}|\nabla\rho|^2\mathrm{d}\mathbf{x} + \varepsilon^2\int_\Omega \rho|\nabla\mathbf{v}|^2\mathrm{d}\mathbf{x} + \int_\Omega \rho|\nabla\mathbf{u}|^2\mathrm{d}\mathbf{x}\Big] + r\int_\Omega \rho|\mathbf{u}|^2\mathrm{d}\mathbf{x} = 0. \tag{1.8}$$

The proof of (1.8) in the case $r = 0$ is available in [20] (see Proposition 10) for the barotropic compressible QNS problem or in [7] (see Proposition 4) for the more general Euler–Korteweg and Navier–Stokes–Korteweg systems. The generalization to $r \neq 0$ is straightforward. We emphasize in particular that, based on the definition of $\mathbf{v}$ in (1.4), the authors have made extensive use of $\nabla\mathbf{v} = \nabla^T\mathbf{v}$.

The main objective of this paper is to propose a Finite-Volume scheme that satisfies a discrete BD-entropy inequality. It should be noted that the discrete counterpart of the continuous inequality (1.8) cannot be guaranteed since, in discrete form, the symmetry of the gradient of $\mathbf{v}$ does not hold. Nevertheless, we propose to reformulate the system (1.1) in terms of variables $(\rho,\mathbf{w},\mathbf{v})$, in order to derive another discrete BD-entropy inequality, such that entropy reduction is also guaranteed in the discrete case. It should be noted that the originality of our contribution compared to [2] and [3] lies in the fact that we derive a discrete BD-entropy inequality instead of an energy inequality. To achieve this goal, the system of equations is reformulated in terms of the variables $(\rho,\mathbf{w},\mathbf{v})$ instead of the variables $(\rho,\mathbf{u},\mathbf{v})$. In the numerical part, several tests are performed to prove the correct behavior of the scheme in several physical and analytical configurations, as well as the consistency of the calculated solutions with those of the initial third-order system (1.1).

The paper layout is as follows. Section 2 is devoted to deriving the new entropy inequality that will replace (1.8), since when the system is discretized, the identity $\nabla\mathbf{v} = \nabla^T\mathbf{v}$ can no longer be used. Although the approach is almost the same as in [20] and [7], the proof is given in a specific form, in order to be used as a guide for the proof in the discrete case. It begins in particular by reformulating the system in terms of variables $(\rho,\mathbf{w},\mathbf{v})$. Next, Section 3 describes the proposed Finite-Volume scheme with the definitions of the discrete operators. It is based on a time splitting, enabling us to deal successively with the hyperbolic and parabolic parts of the system. Section 4 establishes the discrete BD-entropy inequality, leading to the Theorem 4.4 which constitutes the main result of the article. Section 5 is devoted to the special case $d = 1$, for which the BD-entropy inequality can be generalized into a so-called "κ-entropy inequality", see the Corollary 5.2. Finally, Section 6 is devoted to numerical benchmarks, in order to underline the efficiency of the proposed numerical scheme. We first present

some 1D tests from [13], namely the one-dimensional "gray" soliton as well as the dispersive Riemann problem. Next, we propose a 2D benchmark to illustrate the accuracy of the numerical scheme.

2. The continuous BD-entropy equality

2.1. System reformulation

As already mentioned in the introduction, our goal is to provide a numerical scheme designed to approximate the solutions of (1.1), while allowing to obtain a discrete BD-entropy inequality which consists in the discrete counterpart of (1.8). To do it, we first reformulate the system (1.1) in the system (2.1), which constitutes an equivalent one in the $(\rho, \mathbf{w}, \mathbf{v})$ variables:

$$\partial_t \rho + \operatorname{div}(\rho \mathbf{w}) = \nu \Delta \rho, \tag{2.1a}$$

$$\begin{aligned} \partial_t(\rho \mathbf{w}) + \operatorname{div}(\rho \mathbf{w} \otimes \mathbf{w}) + \nabla(p(\rho) + r\nu\rho) = \nu \operatorname{div}(\mathbf{w} \otimes \nabla \rho) + (\varepsilon^2 - \nu^2) \operatorname{div}(\rho \nabla^T \mathbf{v}) \\ + \nu \operatorname{div}(\rho \nabla \mathbf{w}) - r\rho \mathbf{w} + 2r\nu \nabla \rho, \end{aligned} \tag{2.1b}$$

$$\partial_t(\rho \mathbf{v}) + \operatorname{div}(\rho \mathbf{v} \otimes \mathbf{w}) = \nu \operatorname{div}(\mathbf{v} \otimes \nabla \rho) - \operatorname{div}(\rho \nabla^T \mathbf{w}) + \nu \operatorname{div}(\rho \nabla \mathbf{v}), \tag{2.1c}$$

$$\rho_{|t=0} = \rho_0, \qquad (\rho \mathbf{w})_{|t=0} = \rho_0 \mathbf{w}_0, \qquad (\rho \mathbf{v})_{|t=0} = \rho_0 \mathbf{v}_0. \tag{2.1d}$$

Let us note that equation (2.1c) is nothing else but the gradient of equation (2.1a). Introducing this new unknown $\mathbf{v}$ allows to decrease the degree of the system, and to obtain a second-order system easier to solve from the numerical point of view. From the definition of $\mathbf{v}$ in (1.4), we also replace $\nabla \mathbf{v}$ by $\nabla^T \mathbf{v}$ in (2.1b) and $\nabla^T \mathbf{v}$ by $\nabla \mathbf{v}$ in (2.1c). Moreover, let us note that we could substract the value of $r\nu\nabla\rho$ in the left and in the right-hand sides of equation (2.1b), since it appears in both of them. Nevertheless, for numerical reasons to be explained later (see Remark 2.3 below), the system (2.1) is left in this form.

2.2. Continuous BD-entropy equality

The system (2.1a)–(2.1b)–(2.1c) takes the formulation:

$$\partial_t U + \operatorname{div} F(U) = \operatorname{div} M(U) + S(U) \tag{2.2}$$

where

$$U = \begin{bmatrix} \rho \\ \rho \mathbf{w} \\ \rho \mathbf{v} \end{bmatrix}, \quad F(U) = \begin{bmatrix} \rho \mathbf{w} \\ \rho \mathbf{w} \otimes \mathbf{w} + p(\rho) \mathbb{I}_d + r\nu\rho \mathbb{I}_d \\ \rho \mathbf{v} \otimes \mathbf{w} \end{bmatrix}, \quad S(U) = \begin{bmatrix} 0 \\ -r\rho \mathbf{w} + 2r\nu \nabla \rho \\ 0 \end{bmatrix},$$

and

$$M(U) = M_1(U) + M_2(U),$$

with

$$M_1(U) = \begin{bmatrix} 0 \\ (\varepsilon^2 - \nu^2)\rho \nabla^T \mathbf{v} + \nu\rho \nabla \mathbf{w} \\ \nu\rho \nabla \mathbf{v} - \rho \nabla^T \mathbf{w} \end{bmatrix} \quad \text{and} \quad M_2(U) = \nu \begin{bmatrix} \nabla \rho \\ \mathbf{w} \otimes \nabla \rho \\ \mathbf{v} \otimes \nabla \rho \end{bmatrix}. \tag{2.3}$$

We give now the proof of the entropy equality (1.8), by a specific way which will be used as a guideline for the discrete developments in Section 4.

Lemma 2.1. *Suppose that* $(\rho, \mathbf{w}, \mathbf{v})$ *is a strong enough solution of* (2.2) *and that the entropy* E_ε *is defined by* (1.6)–(1.7)*. Then, we have*

$$\frac{\mathrm{d}E_\varepsilon}{\mathrm{d}t}(\rho,\mathbf{v},\mathbf{w}) + \nu\Big[\int_\Omega \gamma\rho^{\gamma-2}|\nabla\rho|^2\mathrm{d}\mathbf{x} + \varepsilon^2\int_\Omega \rho|\nabla\mathbf{v}|^2\mathrm{d}\mathbf{x} + \int_\Omega \rho|\nabla\mathbf{w} - \nu\nabla^T\mathbf{v}|^2\mathrm{d}\mathbf{x}\Big] + r\int_\Omega \rho|\mathbf{w}-\nu\mathbf{v}|^2\mathrm{d}\mathbf{x} = 0. \quad (2.4)$$

Proof. Without loss of generality, the proof is given for $d = 2$. Defining $U = [U_1, U_2, U_3, U_4, U_5]^T = [\rho, \rho w_1, \rho w_2, \rho v_1, \rho v_2]^T$, we first observe that:

$$\nabla_U e_\varepsilon(U) = \begin{pmatrix} -\frac{U_2^2+U_3^2+(\epsilon^2+\nu^2)(U_4^2+U_5^2)}{2U_1^2} + \frac{\gamma U_1^{\gamma-1}}{\gamma-1} + r\nu(1+\log(U_1)) \\ U_2/U_1 \\ U_3/U_1 \\ (\epsilon^2+\nu^2)U_4/U_1 \\ (\epsilon^2+\nu^2)U_5/U_1 \end{pmatrix}. \quad (2.5)$$

Then, we define F_1 and F_2 by

$$F_1(U) = \begin{bmatrix} U_2 \\ U_2^2/U_1 + U_1^\gamma + r\nu U_1 \\ U_2U_3/U_1 \\ U_2U_4/U_1 \\ U_2U_5/U_1 \end{bmatrix} \quad \text{and} \quad F_2(U) = \begin{bmatrix} U_3 \\ U_2U_3/U_1 \\ U_3^2/U_1 + U_1^\gamma + r\nu U_1 \\ U_3U_4/U_1 \\ U_3U_5/U_1 \end{bmatrix}, \quad (2.6)$$

so that $\operatorname{div} F(U) = \partial_1 F_1(U) + \partial_2 F_2(U)$. We also define G_1 and G_2 by:

$$G_1(U) = \frac{U_2}{U_1}(e_\varepsilon(U) + U_1^\gamma + r\nu U_1) \quad \text{and} \quad G_2(U) = \frac{U_3}{U_1}(e_\varepsilon(U) + U_1^\gamma + r\nu U_1). \quad (2.7)$$

Then it can be easily proved that:

$$(\nabla_U e_\varepsilon(U))^T \nabla_U F_i(U) = (\nabla_U G_i(U))^T \qquad \text{for } i = 1, 2, \quad (2.8)$$

leading to:

$$(\nabla_U e_\varepsilon(U))^T \operatorname{div} F(U) = \operatorname{div} G(U),$$

so that:

$$\int_\Omega (\nabla_U e_\varepsilon(U))^T \operatorname{div} F(U)\mathrm{d}\mathbf{x} = 0. \quad (2.9)$$

Now we have :

$$\begin{aligned}
&\int_\Omega (\nabla_U e_\varepsilon(U))^T \operatorname{div} M_1(U)\mathrm{d}\mathbf{x} \\
&\quad = \int_\Omega \Big\{ \Big[(\epsilon^2-\nu^2)\operatorname{div}(\rho\nabla^T\mathbf{v}) + \nu\operatorname{div}(\rho\nabla\mathbf{w})\Big]\cdot\mathbf{w} + (\epsilon^2+\nu^2)\Big[\nu\operatorname{div}(\rho\nabla\mathbf{v}) - \operatorname{div}(\rho\nabla^T\mathbf{w})\Big]\cdot\mathbf{v}\Big\}\mathrm{d}\mathbf{x} \\
&\quad = \int_\Omega \Big\{ (\epsilon^2-\nu^2)\operatorname{div}(\rho\nabla^T\mathbf{v})\cdot\mathbf{w} - \nu\rho|\nabla\mathbf{w}|^2 - (\epsilon^2+\nu^2)\Big[\nu\rho|\nabla\mathbf{v}|^2 + \operatorname{div}(\rho\nabla^T\mathbf{w})\cdot\mathbf{v}\Big]\Big\}\mathrm{d}\mathbf{x}.
\end{aligned}$$

Using the usual notation $\mathbf{A} : \mathbf{B} = \sum_{i,j} \mathbf{A}_{i,j}\mathbf{B}_{j,i}$ so that $\mathbf{A} : \mathbf{A}^T = \sum_{i,j} \mathbf{A}_{ij}^2 = |\mathbf{A}|^2$ is the square of the Frobenius norm, we have:

$$\int_\Omega \operatorname{div}(\rho\nabla^T\mathbf{w})\cdot\mathbf{v}\mathrm{d}\mathbf{x} = -\int_\Omega \rho\nabla^T\mathbf{w} : \nabla^T\mathbf{v}\mathrm{d}\mathbf{x} = \int_\Omega \mathbf{w}\cdot\operatorname{div}(\rho\nabla^T\mathbf{v})\mathrm{d}\mathbf{x}. \quad (2.10)$$

Consequently we obtain:

$$\begin{aligned}\int_\Omega (\nabla_U e_\varepsilon(U))^T \operatorname{div} M_1(U)\mathrm{d}\mathbf{x}&\\ &= \int_\Omega \Big\{ -\nu\rho\varepsilon^2|\nabla\mathbf{v}|^2 - \nu\rho\Big(|\nabla\mathbf{w}|^2+\nu^2|\nabla^T\mathbf{v}|^2\Big) - 2\nu^2\operatorname{div}(\rho\nabla^T\mathbf{v})\cdot\mathbf{w}\Big\}\mathrm{d}\mathbf{x}\\ &= \int_\Omega \Big\{ -\nu\rho\varepsilon^2|\nabla\mathbf{v}|^2 - \nu\rho\Big(|\nabla\mathbf{w}|^2+\nu^2|\nabla^T\mathbf{v}|^2 - 2\nu\nabla^T\mathbf{v}:\nabla^T\mathbf{w}\Big)\Big\}\mathrm{d}\mathbf{x}\\ &= \int_\Omega \Big\{ -\nu\rho\varepsilon^2|\nabla\mathbf{v}|^2 - \nu\rho\big|\nabla\mathbf{w}-\nu\nabla^T\mathbf{v}\big|^2\Big\}\mathrm{d}\mathbf{x}. \qquad (2.11)\end{aligned}$$

Moreover:

$$\begin{aligned}\int_\Omega (\nabla_U e_\varepsilon(U))^T \operatorname{div} M_2(U)\mathrm{d}\mathbf{x}&\\ &= \int_\Omega\Big\{\Big[-\frac{1}{2}\Big(|\mathbf{w}|^2+(\epsilon^2+\nu^2)|\mathbf{v}|^2\Big)+\frac{\gamma}{\gamma-1}\rho^{\gamma-1}+r\nu(1+\log(\rho))\Big]\nu\Delta\rho\\ &\qquad +\nu\operatorname{div}(\mathbf{w}\otimes\nabla\rho)\cdot\mathbf{w}+\nu(\epsilon^2+\nu^2)\operatorname{div}(\mathbf{v}\otimes\nabla\rho)\cdot\mathbf{v}\Big\}\mathrm{d}\mathbf{x}.\end{aligned}$$

Using now the fact that for any $\mathbf{a}\in\mathbb{R}^2$ we have:

$$\int_\Omega(\operatorname{div}(\mathbf{a}\otimes\nabla\rho))\cdot\mathbf{a}\mathrm{d}\mathbf{x}=\frac{1}{2}\int_\Omega|\mathbf{a}|^2\Delta\rho\mathrm{d}\mathbf{x},$$

we obtain:

$$\begin{aligned}\int_\Omega (\nabla_U e_\varepsilon(U))^T \operatorname{div} M_2(U)\mathrm{d}\mathbf{x} &= \int_\Omega\Big\{-\frac{\nu\Delta\rho}{2}\Big(|\mathbf{w}|^2+(\epsilon^2+\nu^2)|\mathbf{v}|^2\Big)-\nu\gamma\rho^{\gamma-2}|\nabla\rho|^2\\ &\qquad -r\nu^2\rho\Big|\frac{\nabla\rho}{\rho}\Big|^2+\frac{\nu}{2}\int_\Omega|\mathbf{w}|^2\Delta\rho+\nu(\epsilon^2+\nu^2)\int_\Omega|\mathbf{v}|^2\Delta\rho\Big\}\mathrm{d}\mathbf{x}\\ &= \int_\Omega\{-\nu\gamma\rho^{\gamma-2}|\nabla\rho|^2-r\nu^2\rho|\mathbf{v}|^2\}\mathrm{d}\mathbf{x}. \qquad (2.12)\end{aligned}$$

Now, it remains to evaluate:

$$\begin{aligned}\int_\Omega(\nabla_U e_\varepsilon(U))^T S(U)\mathrm{d}\mathbf{x} &= \int_\Omega\Big\{-r\rho\mathbf{w}+2r\nu\rho\frac{\nabla\rho}{\rho}\Big\}\cdot\mathbf{w}\mathrm{d}\mathbf{x}\\ &= \int_\Omega -r\rho\Big\{\Big|\mathbf{w}-\nu\frac{\nabla\rho}{\rho}\Big|^2+\nu^2\Big|\frac{\nabla\rho}{\rho}\Big|^2\Big\}\mathrm{d}\mathbf{x}\\ &= \int_\Omega -r\rho\{|\mathbf{w}-\nu\mathbf{v}|^2-\nu^2|\mathbf{v}|^2\}\mathrm{d}\mathbf{x}. \qquad (2.13)\end{aligned}$$

From (2.11), (2.12) and (2.13), we obtain:

$$\begin{aligned}\int_\Omega(\nabla_U e_\varepsilon(U))^T(\operatorname{div}M(U)+S(U))\mathrm{d}\mathbf{x}&\\ &= -\int_\Omega\Big\{\nu\gamma\rho^{\gamma-2}|\nabla\rho|^2+\nu\rho\varepsilon^2|\nabla\mathbf{v}|^2+\nu\rho|\nabla\mathbf{w}-\nu\nabla^T\mathbf{v}|^2+r\rho|\mathbf{w}-\nu\mathbf{v}|^2\Big\}\mathrm{d}\mathbf{x}. \qquad (2.14)\end{aligned}$$

Finally, from (2.2), (2.9) and (2.14) we have:

$$\int_\Omega(\nabla_U e_\varepsilon(U))^T\partial_t U\mathrm{d}\mathbf{x}=-\int_\Omega\Big\{\nu\gamma\rho^{\gamma-2}|\nabla\rho|^2+\nu\rho\varepsilon^2|\nabla\mathbf{v}|^2+\nu\rho|\nabla\mathbf{w}-\nu\nabla^T\mathbf{v}|^2+r\rho|\mathbf{w}-\nu\mathbf{v}|^2\Big\}\mathrm{d}\mathbf{x},$$

so that (2.4) holds. ∎

Remark 2.2. Clearly, in the continuous case, definitions (1.4) and (1.5) and the symmetry of the gradient of $\mathbf{v}$ allow us to obtain the equivalence between (2.4) and (1.8). But in the discrete case $\nabla^T \mathbf{v} \neq \nabla \mathbf{v}$, which is why we leave the result of Lemma 2.1 written in this form.

Remark 2.3. Let us note that the addition of $r\nu\rho\mathbb{I}_d$ in the second component of $F(U)$ - and, consequently, the addition of $r\nu\nabla\rho$ in the second component of $S(U)$ - is necessary to obtain the entropy - entropy flow pair (2.8).

3. The finite volume scheme

In this section, we aim to define a finite volume scheme for the numerical approximation of the solutions of (2.1) in the case $d = 2$ where $\Omega = [a, b] \times [c, d]$ is a rectangle and where system (2.2) is considered with periodic boundary conditions. For $(N_1, N_2) \in (\mathbb{N}^*)^2$ we define $h_1 = (b - a)/N_1$ and $h_2 = (d - c)/N_2$. We then define h and the regularity-mesh coefficient τ as

$$h = \max(h_1, h_2) \text{ and } \tau = \max\left(\frac{h_1}{h_2}, \frac{h_2}{h_1}\right), \tag{3.1}$$

where τ is supposed to be uniformly bounded when the mesh is being refined. For $N_T \in \mathbb{N}^*$, we define $\Delta t = T/N_T$ and $t_n = n\Delta t$, $0 \leq n \leq N_T$. The unknown $\alpha^n_{i,j}$ is the approximated value of $\alpha(t_n, X_{i,j})$ with $X_{i,j} = ((x_1)_i, (x_2)_j)^T$, $(x_1)_i = ih_1 - h_1/2$ $(1 \leq i \leq N_1)$ and $(x_2)_j = jh_2 - h_2/2$ $(1 \leq j \leq N_2)$.

3.1. Time integration

From the knowledge of U^n corresponding to the time approximation of $U(t_n)$, we define U^{n+1} by considering two successive steps, following the same principle as in [2, 3].

First, the hyperbolic step, which is explicit :

$$\frac{U^{n+\frac{1}{2}} - U^n}{\Delta t} + \operatorname{div}(F(U^n)) = 0. \tag{3.2}$$

Then, the parabolic step associated to the source term, which is implicit :

$$\frac{U^{n+1} - U^{n+\frac{1}{2}}}{\Delta t} = \operatorname{div} M(U^{n+1}) + S(U^{n+1}). \tag{3.3}$$

Let us note that the parabolic step (3.3) remains linear. Indeed, according to the first component of U^{n+1}, $S(U^{n+1})$ and $M(U^{n+1})$, the computation of ρ^{n+1} can be done independently of the other part of the system.

3.2. Hyperbolic step

The hyperbolic step (3.2) is computed with the use of a classical Rusanov scheme, namely:

$$U^{n+\frac{1}{2}}_{i,j} = U^n_{i,j} - \Delta t\left(\frac{(F_1)^n_{i+\frac{1}{2},j} - (F_1)^n_{i-\frac{1}{2},j}}{h_1} + \frac{(F_2)^n_{i,j+\frac{1}{2}} - (F_2)^n_{i,j-\frac{1}{2}}}{h_2}\right), \quad 1 \leq i \leq N_1, 1 \leq j \leq N_2 \tag{3.4}$$

with

$$(F_1)^n_{i+\frac{1}{2},j} = \frac{F_1(U^n_{i,j}) + F_1(U^n_{i+1,j})}{2} - \left(\max_{k\in\{i,i+1\}} (c_1)^n_{k,j}\right)\left(\frac{U^n_{i+1,j} - U^n_{i,j}}{2}\right),$$

$$(F_2)^n_{i,j+\frac{1}{2}} = \frac{F_2(U^n_{i,j}) + F_2(U^n_{i,j+1})}{2} - \left(\max_{k\in\{j,j+1\}} (c_2)^n_{i,k}\right)\left(\frac{U^n_{i,j+1} - U^n_{i,j}}{2}\right),$$

with

$$(c_1)^n_{k,j} = \left(\left| \frac{(U_2)^n_{k,j}}{(U_1)^n_{k,j}} \right| + \sqrt{\gamma((U_1)^n_{k,j})^{\gamma-1} + r\nu} \right), \quad (c_2)^n_{i,k} = \left(\left| \frac{(U_3)^n_{i,k}}{(U_1)^n_{i,k}} \right| + \sqrt{\gamma((U_1)^n_{i,k})^{\gamma-1} + r\nu} \right),$$

and where F_1 and F_2 are defined by (2.6). The stability of the scheme is ensured under the CFL condition

$$c\Delta t \leq h, \tag{3.5}$$

with

$$c = \max_{i,j} \{ \max\{(c_1)^n_{i,j}, (c_2)^n_{i,j}\} \} \quad \text{and} \quad h = \min(h_1, h_2).$$

Let us note that under the CFL condition (3.5), the positivity of $\rho^{n+\frac{1}{2}}$ is ensured.

3.3. **Parabolic step**

3.3.1. *Operators definitions and numerical scheme*

In order to define the numerical scheme devoted to the parabolic step, we define some generic discrete operators, where in the following $\alpha_{i,j}$ and $\beta_{i,j}$ are discrete scalar quantities, and $\mathbf{a}_{i,j} = ((a_1)_{i,j}, (a_2)_{i,j})^T$ a discrete vectorial one, $1 \leq i \leq N_1$, $1 \leq j \leq N_2$:

$$\alpha_{i+\frac{1}{2},j} = \frac{\alpha_{i,j} + \alpha_{i+1,j}}{2}, \qquad \alpha_{i,j+\frac{1}{2}} = \frac{\alpha_{i,j} + \alpha_{i,j+1}}{2} \tag{3.6}$$

$$\widetilde{\alpha}_{i+\frac{1}{2},j} = \sqrt{\alpha_{i+\frac{1}{2},j}\alpha_{i+1,j-\frac{1}{2}}}, \qquad \widetilde{\alpha}_{i,j+\frac{1}{2}} = \sqrt{\alpha_{i,j+\frac{1}{2}}\alpha_{i-\frac{1}{2},j+1}} \tag{3.7}$$

$$(\delta_1\alpha)_{i+\frac{1}{2},j} = \alpha_{i+1,j} - \alpha_{i,j}, \qquad (\delta_2\alpha)_{i,j+\frac{1}{2}} = \alpha_{i,j+1} - \alpha_{i,j}$$

$$(\partial_1(\alpha\partial_1\beta))_{i,j} = \frac{\alpha_{i+\frac{1}{2},j}(\delta_1\beta)_{i+\frac{1}{2},j} - \alpha_{i-\frac{1}{2},j}(\delta_1\beta)_{i-\frac{1}{2},j}}{h_1^2} \tag{3.8}$$

$$(\partial_2(\alpha\partial_2\beta))_{i,j} = \frac{\alpha_{i,j+\frac{1}{2}}(\delta_2\beta)_{i,j+\frac{1}{2}} - \alpha_{i,j-\frac{1}{2}}(\delta_2\beta)_{i,j-\frac{1}{2}}}{h_2^2} \tag{3.9}$$

$$(\partial_2(\alpha\partial_1\beta))_{i-\frac{1}{2},j+\frac{1}{2}} = \frac{\widetilde{\alpha}_{i-\frac{1}{2},j+1}(\delta_1\beta)_{i-\frac{1}{2},j+1} - \widetilde{\alpha}_{i-\frac{1}{2},j}(\delta_1\beta)_{i-\frac{1}{2},j}}{h_1 h_2} \tag{3.10}$$

$$(\partial_1(\alpha\partial_2\beta))_{i+\frac{1}{2},j-\frac{1}{2}} = \frac{\widetilde{\alpha}_{i+1,j-\frac{1}{2}}(\delta_2\beta)_{i+1,j-\frac{1}{2}} - \widetilde{\alpha}_{i,j-\frac{1}{2}}(\delta_2\beta)_{i,j-\frac{1}{2}}}{h_1 h_2} \tag{3.11}$$

$$\mathrm{div}(\nabla\alpha)_{i,j} = (\Delta\alpha)_{i,j} = \left[\frac{(\delta_1\alpha)_{i+\frac{1}{2},j} - (\delta_1\alpha)_{i-\frac{1}{2},j}}{h_1^2} + \frac{(\delta_2\alpha)_{i,j+\frac{1}{2}} - (\delta_2\alpha)_{i,j-\frac{1}{2}}}{h_2^2} \right] \tag{3.12}$$

$$\mathrm{div}(\mathbf{a} \otimes \nabla\alpha)_{i,j} = \begin{pmatrix} \partial_1(a_1\partial_1\alpha)_{i,j} + \partial_2(a_1\partial_2\alpha)_{i,j} \\ \partial_1(a_2\partial_1\alpha)_{i,j} + \partial_2(a_2\partial_2\alpha)_{i,j} \end{pmatrix} \tag{3.13}$$

$$\mathrm{div}(\alpha\nabla\mathbf{a})_{i,j} = \begin{pmatrix} \partial_1(\alpha\partial_1 a_1)_{i,j} + \partial_2(\alpha\partial_2 a_1)_{i,j} \\ \partial_1(\alpha\partial_1 a_2)_{i,j} + \partial_2(\alpha\partial_2 a_2)_{i,j} \end{pmatrix} \tag{3.14}$$

$$\mathrm{div}(\alpha\nabla^T\mathbf{a})_{i,j} = \begin{pmatrix} \partial_1(\alpha\partial_1 a_1)_{i,j} + \partial_2(\alpha\partial_1 a_2)_{i-\frac{1}{2},j+\frac{1}{2}} \\ \partial_1(\alpha\partial_2 a_1)_{i+\frac{1}{2},j-\frac{1}{2}} + \partial_2(\alpha\partial_2 a_2)_{i,j} \end{pmatrix}. \tag{3.15}$$

The discretization of $\nabla\rho$ arising in the definition of $S(U)$ is given by:

$$(\nabla\rho)_{i,j} = \left(\sqrt{\frac{\rho_{i,j}}{\widehat{\rho}_{i-\frac{1}{2},j}}} \frac{(\delta_1\rho)_{i-\frac{1}{2},j}}{h_1}, \quad \sqrt{\frac{\rho_{i,j}}{\widehat{\rho}_{i,j-\frac{1}{2}}}} \frac{(\delta_2\rho)_{i,j-\frac{1}{2}}}{h_2} \right)^T, \tag{3.16}$$

where $\widehat{\rho}_{i-\frac{1}{2},j} \in]\rho_{i-1,j}, \rho_{i,j}[$ and $\widehat{\rho}_{i,j-\frac{1}{2}} \in]\rho_{i,j-1}, \rho_{i,j}[$ are defined by:

$$\widehat{\rho}_{i-\frac{1}{2},j} = \frac{\rho_{i,j} - \rho_{i-1,j}}{\log(\rho_{i,j}) - \log(\rho_{i-1,j})} \quad \text{and} \quad \widehat{\rho}_{i,j-\frac{1}{2}} = \frac{\rho_{i,j} - \rho_{i,j-1}}{\log(\rho_{i,j}) - \log(\rho_{i,j-1})}. \tag{3.17}$$

Finally, for the discretization of the pressure term we define $\widetilde{\rho}_{i-\frac{1}{2},j} \in]\rho_{i-1,j}, \rho_{i,j}[$ and $\widetilde{\rho}_{i,j-\frac{1}{2}} \in]\rho_{i,j-1}, \rho_{i,j}[$ respectively by:

$$\widetilde{\rho}^{\gamma-2}_{i-\frac{1}{2},j} = \frac{1}{(\gamma-1)} \frac{\rho^{\gamma-1}_{i,j} - \rho^{\gamma-1}_{i-1,j}}{\rho_{i,j} - \rho_{i-1,j}} \quad \text{and} \quad \widetilde{\rho}^{\gamma-2}_{i,j-\frac{1}{2}} = \frac{1}{(\gamma-1)} \frac{\rho^{\gamma-1}_{i,j} - \rho^{\gamma-1}_{i,j-1}}{\rho_{i,j} - \rho_{i,j-1}}. \tag{3.18}$$

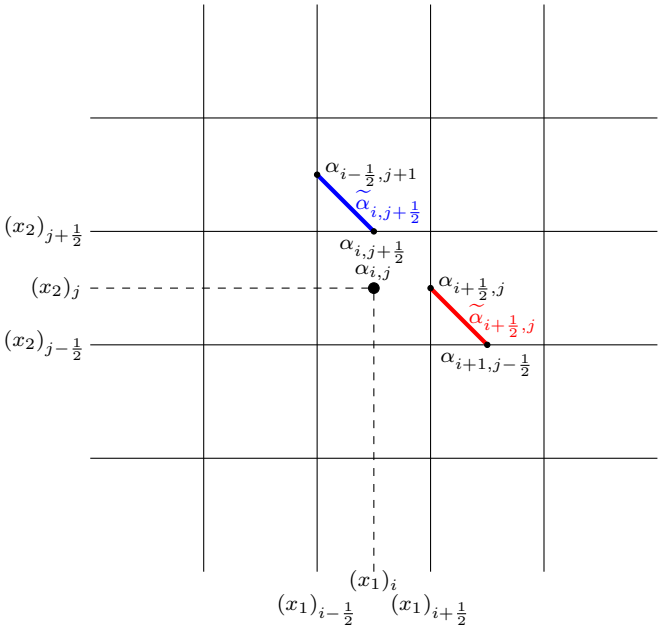

FIGURE 3.1. Notations for the discrete scalar quantities corresponding to (3.6) and (3.7).

Remark 3.1. While the discretizations (3.8) and (3.9) are rather classical and expected, the discretizations (3.10) and (3.11) arising in (3.15) are less so. In the particular case where α is constant, it can be easily shown that (3.10) (resp. (3.11)) corresponds to a discretization of the continuous operators at point $X_{i-\frac{1}{2},j+\frac{1}{2}}$ (resp. at point $X_{i+\frac{1}{2},j-\frac{1}{2}}$) to order $\mathcal{O}(h^2)$. If α is not constant, we introduce the geometric mean given by (3.7) (see Figure 3.1 where $\widetilde{\alpha}_{i+\frac{1}{2},j}$ (resp. $\widetilde{\alpha}_{i,j+\frac{1}{2}}$) belongs to the red (resp. blue) line). As we shall see, this choice is necessary to derive the discrete entropy inequality. In Appendix A we show that (3.10) and (3.11) correspond to discretizations of the continuous operators at point $X_{i,j}$ to order $\mathcal{O}(h)$. Another possibility, instead of (3.10) and (3.11), would have been for example the more

expected one, similar to the one in Section 3.2 of [2] but on a smaller stencil:

$$(\partial_2(\alpha\partial_1\beta))_{i-\frac{1}{2},j+\frac{1}{2}} = \frac{\alpha_{i-\frac{1}{2},j+1}(\delta_1\beta)_{i-\frac{1}{2},j+1} - \alpha_{i-\frac{1}{2},j}(\delta_1\beta)_{i-\frac{1}{2},j}}{h_1h_2},$$
$$(\partial_1(\alpha\partial_2\beta))_{i+\frac{1}{2},j-\frac{1}{2}} = \frac{\alpha_{i+1,j-\frac{1}{2}}(\delta_2\beta)_{i+1,j-\frac{1}{2}} - \alpha_{i,j-\frac{1}{2}}(\delta_2\beta)_{i,j-\frac{1}{2}}}{h_1h_2}.$$

Nevertheless, with such a choice it would not have been possible to obtain (4.10) in the proof of Lemma 4.3 (see below). Moreover, as we shall see, the way to discretize the gradient of the density in (3.16) is also necessary to derive the discrete entropy inequality.

We can now define the numerical scheme allowing to perform the parabolic step (3.3). First of all, the value of ρ^{n+1} is computed by solving the heat equation, which corresponds to the first component of (3.3):

$$\rho_{i,j}^{n+1} - \nu\Delta t(\Delta\rho)_{i,j}^{n+1} = \rho_{i,j}^{n+\frac{1}{2}}, \quad 1 \le i \le N_1, 1 \le j \le N_2. \tag{3.19}$$

Then, we solve the remaining system in order to compute $\mathbf{w}_{i,j}^{n+1}$ and $\mathbf{v}_{i,j}^{n+1}$, $1 \le i \le N_1, 1 \le j \le N_2$:

$$\rho_{i,j}^{n+1}\mathbf{w}_{i,j}^{n+1} - \Delta t\Big[(\varepsilon^2-\nu^2)\operatorname{div}(\rho^{n+1}\nabla^T\mathbf{v}^{n+1})_{i,j} + \nu\operatorname{div}(\rho^{n+1}\nabla\mathbf{w}^{n+1})_{i,j} + \nu\operatorname{div}(\mathbf{w}^{n+1}\otimes\nabla\rho^{n+1})_{i,j} - r\rho_{i,j}^{n+1}\mathbf{w}_{i,j}^{n+1}\Big] = \rho_{i,j}^{n+\frac{1}{2}}\mathbf{w}_{i,j}^{n+\frac{1}{2}} + 2r\nu(\nabla\rho^{n+1})_{i,j} \tag{3.20a}$$

$$\rho_{i,j}^{n+1}\mathbf{v}_{i,j}^{n+1} - \Delta t\Big[\nu\operatorname{div}(\rho^{n+1}\nabla\mathbf{v}^{n+1})_{i,j} - \operatorname{div}(\rho^{n+1}\nabla^T\mathbf{w}^{n+1})_{i,j} + \nu\operatorname{div}(\mathbf{v}^{n+1}\otimes\nabla\rho^{n+1})_{i,j}\Big] = \rho_{i,j}^{n+\frac{1}{2}}\mathbf{v}_{i,j}^{n+\frac{1}{2}} \tag{3.20b}$$

Remark 3.2. Note the presence of terms in ∇^T in (3.20) that correspond to the discretization of $M_1(U)$ in (2.3). According to [7] (see (24)–(25)–(26)), we can read the term $\nabla^T\mathbf{u} = \nabla^T\mathbf{w} - \nu\nabla^T\mathbf{v}$ in the equation for $\mathbf{v}$. In Lemma 4.3 below, we will see that the term $\nabla^T\mathbf{w}$ in (3.20b) cancels out with $\nabla^T\mathbf{v}$ in (3.20a). This could not be done if we had left $\nabla\mathbf{v}$, as in the original system. Finally, replacing $\nabla\mathbf{v}$ with $\nabla^T\mathbf{v}$ in (3.20b) would prevent us from obtaining the Frobenius norm $|\nabla\mathbf{v}|^2$ in the discrete counterpart. This is why we did not leave $\nabla^T\mathbf{v}$, as in the original augmented system.

Remark 3.3. The matrix M of the linear system (3.20), expressed in term of $\rho^{n+1}, \nabla\rho^{n+1}, \nu, \varepsilon$ and r, takes the following form:

$$M = I + \Delta tC. \tag{3.21}$$

In the case $\nu = 0$, corresponding to the quantum Euler equation, we can show that C is similar to an anti-symmetric matrix. Consequently, the real part of all the eigenvalues of M is equal to 1, so that M is invertible. In the case $\nu > 0$, according to (3.21) it is clear that M is invertible provided that Δt is sufficiently small. Note that in the case $\varepsilon > \nu > 0$, numerical simulations suggest that, as in the case $\nu = 0$, the real part of all the eigenvalues of M always remains larger or equal to 1 (see Appendix B), so that M is invertible. As explained in [1] (see Corollary 1.2), this regime corresponds to the case for which the wave energy of a quantum particle with a given frequency in the BGK model is larger than the kinetic energy of a particle which crosses the domain in time $1/\omega$. Consequently, the configuration $\varepsilon > \nu > 0$ corresponds to an upper bound for the collision frequency, which is physically meaningful to preserve the quantum behavior of the particles.

4. The discrete entropy inequality

4.1. Hyperbolic step

Let us define the discrete BD-entropy $E_\varepsilon^{(dis)}$ by:

$$E_\varepsilon^{(dis)}(U) = h_1 h_2 \sum_{i,j} e_\varepsilon(U_{i,j}),$$

where e_ε is defined pointwise by (1.7).

Lemma 4.1. *Suppose that $U^{n+\frac{1}{2}}$ is defined by (3.4). Then we have:*

$$E_\varepsilon^{(dis)}(U^{n+\frac{1}{2}}) \leq E_\varepsilon^{(dis)}(U^n). \tag{4.1}$$

Proof. Defining $G_1(U)$ and $G_2(U)$ by (2.7) and thanks to (2.8), it il clear that (e_ε, G) constitutes an entropy - entropy flow pair. Consequently, under the CFL condition (3.5), the Rusanov scheme (3.4) is entropy dissipative, in the sense that it satisfies the following discrete entropy inequality:

$$e_\varepsilon(U_{i,j}^{n+\frac{1}{2}}) \leq e_\varepsilon(U_{i,j}^n) - \Delta t \left(\frac{G_1(U_{i+\frac{1}{2},j}^n) - G_1(U_{i-\frac{1}{2},j}^n)}{h_1} + \frac{G_2(U_{i,j+\frac{1}{2}}^n) - G_2(U_{i,j-\frac{1}{2}}^n)}{h_2} \right),$$
$$1 \leq i \leq N_1, 1 \leq j \leq N_2,$$

where $G_1(U_{i+\frac{1}{2},j}^n)$ (resp. $G_2(U_{i,j+\frac{1}{2}}^n)$) is the entropy numerical flux associated with $(F_1)_{i+\frac{1}{2},j}^n$ (resp. $(F_2)_{i,j+\frac{1}{2}}^n$). Consequently, and thanks to the periodic boundary conditions, (4.1) holds. ∎

4.2. Parabolic step

We first establish Lemma 4.2, which constitutes the discrete counterpart of (2.10). Let us note that this result is proved in [2], but for another choice of discretization that ours. In particular, their way to evaluate the cross-derivatives is not similar to the choice we did in expressions (3.10) and (3.11).

Lemma 4.2.

$$\sum_{i,j} \mathrm{div}(\rho \nabla^T \mathbf{v})_{i,j} \cdot \mathbf{w}_{i,j} = \sum_{i,j} \mathrm{div}(\rho \nabla^T \mathbf{w})_{i,j} \cdot \mathbf{v}_{i,j}$$

Proof. The proof of Lemma 4.2 is given in Appendix C. ∎

Lemma 4.3. *Suppose that U^{n+1} is defined by (3.19)–(3.20). Then we have :*

$$E_\varepsilon^{(dis)}(U^{n+1}) + \Delta t (T_p(U^{n+1}) + T_{\mathbf{v}}(U^{n+1}) + T_{\mathbf{u}}(U^{n+1}) + T_r(U^{n+1})) \leq E_\varepsilon^{(dis)}(U^{n+\frac{1}{2}}) \tag{4.2}$$

with:

$$T_p(U) = \nu\gamma h_1 h_2 \sum_{i,j} \left[\widetilde{\rho}_{i-\frac{1}{2},j}^{\gamma-2} \left(\frac{(\delta_1 \rho)_{i-\frac{1}{2},j}}{h_1} \right)^2 + \widetilde{\rho}_{i,j-\frac{1}{2}}^{\gamma-2} \left(\frac{(\delta_2 \rho)_{i,j-\frac{1}{2}}}{h_2} \right)^2 \right],$$

$$T_{\mathbf{v}}(U) = \nu\varepsilon^2 h_1 h_2 \sum_{k=1}^{2} \sum_{i,j} \left(\rho_{i-\frac{1}{2},j} \left(\frac{(\delta_1 v_k)_{i-\frac{1}{2},j}}{h_1} \right)^2 + \rho_{i,j-\frac{1}{2}} \left(\frac{(\delta_2 v_k)_{i,j-\frac{1}{2}}}{h_2} \right)^2 \right),$$

$$T_{\mathbf{u}}(U) = \nu h_1 h_2 \sum_{i,j} \Bigg[\rho_{i-\frac{1}{2},j} \left(\frac{(\delta_1 w_1)_{i-\frac{1}{2},j}}{h_1} - \nu \frac{(\delta_1 v_1)_{i-\frac{1}{2},j}}{h_1} \right)^2 + \left(\frac{\sqrt{\rho_{i,j-\frac{1}{2}}}(\delta_2 w_1)_{i,j-\frac{1}{2}}}{h_2} - \nu \frac{\sqrt{\rho_{i-\frac{1}{2},j}}(\delta_1 v_2)_{i-\frac{1}{2},j}}{h_1} \right)^2 + \left(\frac{\sqrt{\rho_{i-\frac{1}{2},j}}(\delta_1 w_2)_{i-\frac{1}{2},j}}{h_1} - \nu \frac{\sqrt{\rho_{i,j-\frac{1}{2}}}(\delta_2 v_1)_{i,j-\frac{1}{2}}}{h_2} \right)^2 + \rho_{i,j-\frac{1}{2}} \left(\frac{(\delta_2 w_2)_{i,j-\frac{1}{2}}}{h_2} - \nu \frac{(\delta_2 v_2)_{i,j-\frac{1}{2}}}{h_2} \right)^2 \Bigg]$$

and

$$T_r(U) = r h_1 h_2 \sum_{i,j} \rho_{i,j} \left[\left((w_1)_{i,j} - \frac{\nu(\delta_1 \rho)_{i-\frac{1}{2},j}}{h_1 \sqrt{\rho_{i,j} \widehat{\rho}_{i-\frac{1}{2},j}}} \right)^2 + \left((w_2)_{i,j} - \frac{\nu(\delta_2 \rho)_{i,j-\frac{1}{2}}}{h_2 \sqrt{\rho_{i,j} \widehat{\rho}_{i,j-\frac{1}{2}}}} \right)^2 \right].$$

Proof. First of all, since e_ε defined by (1.7) is a convex function in the variable U, we have:

$$e_\varepsilon(U_{i,j}^{n+1}) \leq e_\varepsilon(U_{i,j}^{n+\frac{1}{2}}) + (U_{i,j}^{n+1} - U_{i,j}^{n+\frac{1}{2}}) \nabla_U e_\varepsilon(U_{i,j}^{n+1}).$$

Then, from (2.5), (3.19) and (3.20), we have:

$$\sum_{i,j} (U_{i,j}^{n+1} - U_{i,j}^{n+\frac{1}{2}}) \cdot \nabla_U e_\varepsilon(U_{i,j}^{n+1}) = \Delta t \sum_{k=1}^{7} A_k$$

where, neglecting the superscript $n+1$:

$$A_1 = \frac{\nu\gamma}{\gamma - 1} \sum_{i,j} \rho_{i,j}^{\gamma-1} (\Delta\rho)_{i,j}$$

$$A_2 = \nu\varepsilon^2 \sum_{i,j} \operatorname{div}(\rho \nabla \mathbf{v})_{i,j} \cdot \mathbf{v}_{i,j}$$

$$A_3 = \nu \sum_{i,j} \Big(\operatorname{div}(\rho \nabla \mathbf{w})_{i,j} \cdot \mathbf{w}_{i,j} + \nu^2 \operatorname{div}(\rho \nabla \mathbf{v})_{i,j} \cdot \mathbf{v}_{i,j} - \nu \operatorname{div}(\rho \nabla^T \mathbf{v})_{i,j} \cdot \mathbf{w}_{i,j} - \nu \operatorname{div}(\rho \nabla^T \mathbf{w})_{i,j} \cdot \mathbf{v}_{i,j} \Big)$$

$$A_4 = r \sum_{i,j} \left(\nu^2 (\Delta\rho)_{i,j} (1 + \log(\rho_{i,j})) + \sum_{i,j} \mathbf{w}_{i,j} \cdot (-\rho_{i,j} \mathbf{w}_{i,j} + 2\nu (\nabla\rho)_{i,j}) \right)$$

$$A_5 = -\nu \sum_{i,j} \left(\frac{1}{2} (\Delta\rho)_{i,j} |\mathbf{w}_{i,j}|^2 - \operatorname{div}(\mathbf{w} \otimes \nabla\rho)_{i,j} \cdot \mathbf{w}_{i,j} \right)$$

$$A_6 = -\nu(\varepsilon^2 + \nu^2) \sum_{i,j} \left(\frac{1}{2} (\Delta\rho)_{i,j} |\mathbf{v}_{i,j}|^2 - \operatorname{div}(\mathbf{v} \otimes \nabla\rho)_{i,j} \cdot \mathbf{v}_{i,j} \right)$$

$$A_7 = \varepsilon^2 \sum_{i,j} \Big(\operatorname{div}(\rho \nabla^T \mathbf{v})_{i,j} \cdot \mathbf{w}_{i,j} - \operatorname{div}(\rho \nabla^T \mathbf{w})_{i,j} \cdot \mathbf{v}_{i,j} \Big).$$

Now, it remains to evaluate each of the quantities A_k, $1 \le k \le 7$. From the definitions (3.12) and (3.18), we have:

$$\begin{aligned}
A_1 &= \frac{\nu\gamma}{\gamma-1}\sum_{i,j}\rho_{i,j}^{\gamma-1}(\Delta\rho)_{i,j}\\
&= \frac{\nu\gamma}{\gamma-1}\sum_{i,j}\left[\frac{(\delta_1\rho)_{i+\frac12,j}-(\delta_1\rho)_{i-\frac12,j}}{h_1^2}\rho_{i,j}^{\gamma-1}+\frac{(\delta_2\rho)_{i,j+\frac12}-(\delta_2\rho)_{i,j-\frac12}}{h_2^2}\rho_{i,j}^{\gamma-1}\right]\\
&= -\frac{\nu\gamma}{\gamma-1}\sum_{i,j}\left[\frac{(\delta_1\rho)_{i-\frac12,j}(\rho_{i,j}^{\gamma-1}-\rho_{i-1,j}^{\gamma-1})}{h_1^2}+\frac{(\delta_2\rho)_{i,j-\frac12}(\rho_{i,j}^{\gamma-1}-\rho_{i,j-1}^{\gamma-1})}{h_2^2}\right]\\
&= -\nu\gamma\sum_{i,j}\left[\widetilde{\rho}_{i-\frac12,j}^{\gamma-2}\left(\frac{(\delta_1\rho)_{i-\frac12,j}}{h_1}\right)^2+\widetilde{\rho}_{i,j-\frac12}^{\gamma-2}\left(\frac{(\delta_2\rho)_{i,j-\frac12}}{h_2}\right)^2\right]\\
&= -\frac{T_p(U)}{h_1h_2}.
\end{aligned}\tag{4.3}$$

Then we have:

$$\begin{aligned}
A_2 &= \nu\varepsilon^2\sum_{i,j}\operatorname{div}(\rho\nabla\mathbf{v})_{i,j}\cdot\mathbf{v}_{i,j}\\
&= \nu\varepsilon^2\sum_{k=1}^{2}\sum_{i,j}(v_k)_{i,j}\left(\frac{\rho_{i+\frac12,j}(\delta_1v_k)_{i+\frac12,j}-\rho_{i-\frac12,j}(\delta_1v_k)_{i-\frac12,j}}{h_1^2}+\frac{\rho_{i,j+\frac12}(\delta_2v_k)_{i,j+\frac12}-\rho_{i,j-\frac12}(\delta_2v_k)_{i,j-\frac12}}{h_2^2}\right)\\
&= -\nu\varepsilon^2\sum_{k=1}^{2}\sum_{i,j}\left(\rho_{i-\frac12,j}\left(\frac{(\delta_1v_k)_{i-\frac12,j}}{h_1}\right)^2+\rho_{i,j-\frac12}\left(\frac{(\delta_2v_k)_{i,j-\frac12}}{h_2}\right)^2\right)\\
&= -\frac{T_{\mathbf{v}}(U)}{h_1h_2}.
\end{aligned}\tag{4.4}$$

From Lemma 4.2, we have:

$$A_3 = \nu\sum_{i,j}\Big(\operatorname{div}(\rho\nabla\mathbf{w})_{i,j}\cdot\mathbf{w}_{i,j}+\nu^2\operatorname{div}(\rho\nabla\mathbf{v})_{i,j}\cdot\mathbf{v}_{i,j}-2\nu\operatorname{div}(\rho\nabla^T\mathbf{v})_{i,j}\cdot\mathbf{w}_{i,j}\Big).\tag{4.5}$$

We can write:

$$\begin{aligned}
\sum_{i,j}\operatorname{div}(\rho\nabla\mathbf{w})_{i,j}\cdot\mathbf{w}_{i,j} &= \sum_{k=1}^{2}\sum_{i,j}\left[(w_k)_{i,j}\left(\frac{\rho_{i+\frac12,j}(\delta_1w_k)_{i+\frac12,j}-\rho_{i-\frac12,j}(\delta_1w_k)_{i-\frac12,j}}{h_1^2}\right.\right.\\
&\qquad\left.\left.+\ \frac{\rho_{i,j+\frac12}(\delta_2w_k)_{i,j+\frac12}-\rho_{i,j-\frac12}((\delta_2w_k)_{i,j-\frac12}}{h_2^2}\right)\right]\\
&= A_{31}+A_{32}
\end{aligned}\tag{4.6}$$

with

$$A_{31} = -\sum_{i,j}\left(\frac{\rho_{i-\frac12,j}(\delta_1w_1)_{i-\frac12,j}^2}{h_1^2}+\frac{\rho_{i,j-\frac12}(\delta_2w_2)_{i,j-\frac12}^2}{h_2^2}\right)$$

and

$$A_{32} = -\sum_{i,j}\left(\frac{\rho_{i-\frac12,j}(\delta_1w_2)_{i-\frac12,j}^2}{h_1^2}+\frac{\rho_{i,j-\frac12}(\delta_2w_1)_{i,j-\frac12}^2}{h_2^2}\right).$$

Similarly,

$$\nu^2\sum_{i,j}\operatorname{div}(\rho\nabla\mathbf{v})_{i,j}\cdot\mathbf{v}_{i,j} = A_{33}+A_{34}\tag{4.7}$$

with

$$A_{33} = -\nu^2 \sum_{i,j} \left(\frac{\rho_{i-\frac{1}{2},j} (\delta_1 v_1)^2_{i-\frac{1}{2},j}}{h_1^2} + \frac{\rho_{i,j-\frac{1}{2}} (\delta_2 v_2)^2_{i,j-\frac{1}{2}}}{h_2^2} \right)$$

and

$$A_{34} = -\nu^2 \sum_{i,j} \left(\frac{\rho_{i-\frac{1}{2},j} (\delta_1 v_2)^2_{i-\frac{1}{2},j}}{h_1^2} + \frac{\rho_{i,j-\frac{1}{2}} (\delta_2 v_1)^2_{i,j-\frac{1}{2}}}{h_2^2} \right).$$

Moreover,

$$\begin{aligned}
&-2\nu \sum_{i,j} \operatorname{div}(\rho \nabla^T \mathbf{v})_{i,j} \cdot \mathbf{w}_{i,j} \\
&\quad = -2\nu \sum_{i,j} \Bigg[(w_1)_{i,j} \Bigg(\frac{\rho_{i+\frac{1}{2},j} (\delta_1 v_1)_{i+\frac{1}{2},j} - \rho_{i-\frac{1}{2},j} (\delta_1 v_1)_{i-\frac{1}{2},j}}{h_1^2} \\
&\qquad\qquad + \frac{\sqrt{\rho_{i-\frac{1}{2},j+1} \rho_{i,j+\frac{1}{2}}} (\delta_1 v_2)_{i-\frac{1}{2},j+1} - \sqrt{\rho_{i-\frac{1}{2},j} \rho_{i,j-\frac{1}{2}}} (\delta_1 v_2)_{i-\frac{1}{2},j}}{h_1 h_2} \Bigg) \\
&\qquad + (w_2)_{i,j} \Bigg(\frac{\sqrt{\rho_{i+1,j-\frac{1}{2}} \rho_{i+\frac{1}{2},j}} (\delta_2 v_1)_{i+1,j-\frac{1}{2}} - \sqrt{\rho_{i,j-\frac{1}{2}} \rho_{i-\frac{1}{2},j}} (\delta_2 v_1)_{i,j-\frac{1}{2}}}{h_1 h_2} \\
&\qquad\qquad + \frac{\rho_{i,j+\frac{1}{2}} (\delta_2 v_2)_{i,j+\frac{1}{2}} - \rho_{i,j-\frac{1}{2}} (\delta_2 v_2)_{i,j-\frac{1}{2}}}{h_2^2} \Bigg) \Bigg] \\
&\quad = A_{35} + A_{36}
\end{aligned} \tag{4.8}$$

with

$$A_{35} = 2\nu \sum_{i,j} \left(\frac{\rho_{i-\frac{1}{2},j} (\delta_1 w_1)_{i-\frac{1}{2},j} (\delta_1 v_1)_{i-\frac{1}{2},j}}{h_1^2} + \frac{\rho_{i,j-\frac{1}{2}} (\delta_2 w_2)_{i,j-\frac{1}{2}} (\delta_2 v_2)_{i,j-\frac{1}{2}}}{h_2^2} \right)$$

and

$$A_{36} = 2\nu \sum_{i,j} \left(\frac{\sqrt{\rho_{i-\frac{1}{2},j} \rho_{i,j-\frac{1}{2}}} (\delta_1 v_2)_{i-\frac{1}{2},j} (\delta_2 w_1)_{i,j-\frac{1}{2}}}{h_1 h_2} + \frac{\sqrt{\rho_{i-\frac{1}{2},j} \rho_{i,j-\frac{1}{2}}} (\delta_1 w_2)_{i-\frac{1}{2},j} (\delta_2 v_1)_{i,j-\frac{1}{2}}}{h_1 h_2} \right).$$

Consequently, we have

$$\begin{aligned}
&A_{31} + A_{33} + A_{35} \\
&\quad = -\sum_{i,j} \left[\rho_{i-\frac{1}{2},j} \left(\frac{(\delta_1 w_1)_{i-\frac{1}{2},j}}{h_1} - \nu \frac{(\delta_1 v_1)_{i-\frac{1}{2},j}}{h_1} \right)^2 + \rho_{i,j-\frac{1}{2}} \left(\frac{(\delta_2 w_2)_{i,j-\frac{1}{2}}}{h_2} - \nu \frac{(\delta_2 v_2)_{i,j-\frac{1}{2}}}{h_2} \right)^2 \right],
\end{aligned} \tag{4.9}$$

as well as

$$\begin{aligned}
A_{32} + A_{34} + A_{36} = -\sum_{i,j} \Bigg[&\left(\frac{\sqrt{\rho_{i,j-\frac{1}{2}}} (\delta_2 w_1)_{i,j-\frac{1}{2}}}{h_2} - \nu \frac{\sqrt{\rho_{i-\frac{1}{2},j}} (\delta_1 v_2)_{i-\frac{1}{2},j}}{h_1} \right)^2 \\
&+ \left(\frac{\sqrt{\rho_{i-\frac{1}{2},j}} (\delta_1 w_2)_{i-\frac{1}{2},j}}{h_1} - \nu \frac{\sqrt{\rho_{i,j-\frac{1}{2}}} (\delta_2 v_1)_{i,j-\frac{1}{2}}}{h_2} \right)^2 \Bigg].
\end{aligned} \tag{4.10}$$

Finally from (4.5), (4.6), (4.7) and (4.8) we have

$$A_3 = \nu \sum_{k=1}^{6} A_{3k},$$

so that from (4.9) and (4.10) we obtain

$$A_3 = -\frac{T_{\mathbf{u}}(U)}{h_1 h_2}. \tag{4.11}$$

From the definitions (3.16) and (3.17), we have:

$$\begin{aligned}
A_4 &= r\sum_{i,j}(\Delta\rho)_{i,j}\Big(\nu^2(1+\log(\rho_{i,j})\Big) + r\sum_{i,j}\mathbf{w}_{i,j}\cdot(-\rho_{i,j}\mathbf{w}_{i,j} + 2\nu(\nabla\rho)_{i,j}) \\
&= r\sum_{i,j}\Bigg[\nu^2(1+\log(\rho_{i,j}))\left(\frac{(\delta_1\rho)_{i+\frac12,j}-(\delta_1\rho)_{i-\frac12,j}}{h_1^2} + \frac{(\delta_2\rho)_{i,j+\frac12}-(\delta_2\rho)_{i,j-\frac12}}{h_2^2}\right) \\
&\qquad - \rho_{i,j}\Big((w_1)_{i,j}^2 + (w_2)_{i,j}^2\Big) + 2\nu(w_1)_{i,j}\sqrt{\frac{\rho_{i,j}}{\widehat{\rho}_{i-\frac12,j}}}\frac{(\delta_1\rho)_{i-\frac12,j}}{h_1} + 2\nu(w_2)_{i,j}\sqrt{\frac{\rho_{i,j}}{\widehat{\rho}_{i,j-\frac12}}}\frac{(\delta_2\rho)_{i,j-\frac12}}{h_2}\Bigg] \\
&= r\sum_{i,j}\Bigg[-\nu^2\left(\frac{(\delta_1\rho)_{i-\frac12,j}(\log(\rho_{i,j})-\log(\rho_{i-1,j}))}{h_1^2} + \frac{(\delta_2\rho)_{i,j-\frac12}(\log(\rho_{i,j})-\log(\rho_{i,j-1}))}{h_2^2}\right) \\
&\qquad - \rho_{i,j}\Big((w_1)_{i,j}^2 + (w_2)_{i,j}^2\Big) + 2\nu(w_1)_{i,j}\sqrt{\frac{\rho_{i,j}}{\widehat{\rho}_{i-\frac12,j}}}\frac{(\delta_1\rho)_{i-\frac12,j}}{h_1} + 2\nu(w_2)_{i,j}\sqrt{\frac{\rho_{i,j}}{\widehat{\rho}_{i,j-\frac12}}}\frac{(\delta_2\rho)_{i,j-\frac12}}{h_2}\Bigg] \\
&= -r\sum_{i,j}\rho_{i,j}\Bigg[\frac{\nu^2(\delta_1\rho)_{i-\frac12,j}^2}{h_1^2\rho_{i,j}\widehat{\rho}_{i-\frac12,j}} - \frac{2\nu(w_1)_{i,j}(\delta_1\rho)_{i-\frac12,j}}{h_1\sqrt{\rho_{i,j}\widehat{\rho}_{i-\frac12,j}}} + (w_1)_{i,j}^2 \\
&\qquad + \frac{\nu^2(\delta_2\rho)_{i,j-\frac12}^2}{h_2^2\rho_{i,j}\widehat{\rho}_{i,j-\frac12}} - \frac{2\nu(w_2)_{i,j}(\delta_2\rho)_{i,j-\frac12}}{h_2\sqrt{\rho_{i,j}\widehat{\rho}_{i,j-\frac12}}} + (w_2)_{i,j}^2\Bigg] \\
&= -r\sum_{i,j}\rho_{i,j}\left[\left((w_1)_{i,j} - \frac{\nu(\delta_1\rho)_{i-\frac12,j}}{h_1\sqrt{\rho_{i,j}\widehat{\rho}_{i-\frac12,j}}}\right)^2 + \left((w_2)_{i,j} - \frac{\nu(\delta_2\rho)_{i,j-\frac12}}{h_2\sqrt{\rho_{i,j}\widehat{\rho}_{i,j-\frac12}}}\right)^2\right] \\
&= -\frac{T_r(U)}{h_1 h_2}.
\end{aligned} \tag{4.12}$$

We write:

$$\begin{aligned}
&\frac12\sum_{i,j}(\Delta\rho)_{i,j}|\mathbf{w}_{i,j}|^2 \\
&\qquad = -\frac12\sum_{i,j}\left[((w_1)_{i,j}^2 + (w_2)_{i,j}^2)\left(\frac{(\delta_1\rho)_{i-\frac12,j}-(\delta_1\rho)_{i+\frac12,j}}{h_1^2} + \frac{(\delta_2\rho)_{i,j-\frac12}-(\delta_2\rho)_{i,j+\frac12}}{h_2^2}\right)\right] \\
&\qquad = -\frac12\sum_{k=1}^{2}\sum_{i,j}\left[\frac{(\delta_1\rho)_{i-\frac12,j}((w_k)_{i,j}^2-(w_k)_{i-1,j}^2)}{h_1^2} + \frac{(\delta_2\rho)_{i,j-\frac12}((w_k)_{i,j}^2+(w_k)_{i,j-1}^2)}{h_2^2}\right],
\end{aligned} \tag{4.13}$$

and moreover

$$\begin{aligned}
&\operatorname{div}(\mathbf{w}\otimes\nabla\rho)_{i,j}\cdot\mathbf{w}_{i,j}\\
&\quad=\sum_{k=1}^{2}\sum_{i,j}\Bigg[(w_k)_{i,j}\frac{(w_k)_{i+\frac12,j}(\delta_1\rho)_{i+\frac12,j}-(w_k)_{i-\frac12,j}(\delta_1\rho)_{i-\frac12,j}}{h_1^2}\\
&\qquad\qquad+(w_k)_{i,j}\frac{(w_k)_{i,j+\frac12}(\delta_2\rho)_{i,j+\frac12,}-(w_k)_{i,j-\frac12}(\delta_2\rho)_{i,j-\frac12,}}{h_2^2}\Bigg]\\
&\quad=\sum_{k=1}^{2}\sum_{i,j}\left[\frac{(w_k)_{i-\frac12,j}(\delta_1\rho)_{i-\frac12,j}(\delta_1 w_k)_{i-\frac12,j}}{h_1^2}+\frac{(w_k)_{i,j-\frac12}(\delta_2\rho)_{i,j-\frac12}(\delta_2 w_k)_{i,j-\frac12}}{h_2^2}\right]\\
&\quad=-\frac12\sum_{k=1}^{2}\sum_{i,j}\left[\frac{(\delta_1\rho)_{i-\frac12,j}((w_k)_{i,j}^2-(w_k)_{i-1,j}^2)}{h_1^2}+\frac{(\delta_2\rho)_{i,j-\frac12}((w_k)_{i,j}^2-(w_k)_{i,j-1}^2)}{h_2^2}\right].
\end{aligned}\tag{4.14}$$

From (4.13) and (4.14), and similar calculus, we obtain

$$A_5=0\quad\text{and}\quad A_6=0.\tag{4.15}$$

Finally from Lemma 4.2, we get:

$$A_7=0.\tag{4.16}$$

To conclude, from (4.3),(4.4),(4.11),(4.12),(4.15) and (4.16), it is clear that (4.2) holds. ∎

4.3. **Complete scheme**

Theorem 4.4. *Suppose that $U^{n+\frac12}$ is defined by* (3.4)*, U^{n+1} is defined by* (3.19)–(3.20)*, and that the entropy E_ε defined by* (1.6)–(1.7)*. Then we have :*

$$E_\varepsilon^{(dis)}(U^{n+1})+\Delta t(T_p(U^{n+1})+T_{\mathbf{v}}(U^{n+1})+T_{\mathbf{u}}(U^{n+1})+T_r(U^{n+1}))\le E_\varepsilon^{(dis)}(U^n)$$

where $T_p(U),T_{\mathbf{v}}(U),T_{\mathbf{u}}(U)$ and $T_r(U)$ are defined in Lemma 4.3.

Proof. Direct consequence of Lemma 4.1 and 4.3. ∎

5. **The one-dimensional case : the κ-entropy inequality**

In this section, we investigate the particular case $d=1$, where the previous results can be generalized to the so-called "κ-entropy" inequality. Indeed, instead of defining $\mathbf{w}$ as in (1.5), we can for any $\kappa\in(0,1)$ define $\mathbf{w}$ by:

$$\mathbf{w}=\mathbf{u}+2\kappa\nu\mathbf{v}.$$

In this case, the system (2.1) takes the more general formulation:

$$\partial_t\rho+\operatorname{div}(\rho\mathbf{w})=2\kappa\nu\Delta\rho,\tag{5.1a}$$

$$\begin{aligned}
&\partial_t(\rho\mathbf{w})+\operatorname{div}(\rho\mathbf{w}\otimes\mathbf{w}+(p(\rho)+2r\kappa\nu\rho)\mathbb{I}_d)\\
&\qquad=2\nu\kappa\operatorname{div}(\mathbf{w}\otimes\nabla\rho)+2\nu\Big[\operatorname{div}(\rho D(\mathbf{w}))-\kappa\operatorname{div}(\rho\nabla^T\mathbf{w})\Big]+4r\kappa\nu\nabla\rho\\
&\qquad\quad-4\kappa\nu^2\Big[\operatorname{div}(\rho D(\mathbf{v}))-\kappa\operatorname{div}(\rho\nabla^T\mathbf{v})\Big]-r\rho\mathbf{w}+\varepsilon^2\operatorname{div}(\rho\nabla\mathbf{v}),
\end{aligned}\tag{5.1b}$$

$$\partial_t(\rho\mathbf{v})+\operatorname{div}(\rho\mathbf{v}\otimes\mathbf{w})=2\kappa\nu\operatorname{div}(\mathbf{v}\otimes\nabla\rho)-\operatorname{div}(\rho\nabla^T\mathbf{w})+2\kappa\nu\operatorname{div}(\rho\nabla^T\mathbf{v}).\tag{5.1c}$$

A "κ-entropy" inequality can be found. Namely, defining this time the κ-entropy by

$$E_\varepsilon^{(\kappa)}(\rho,\mathbf{v},\mathbf{w})=\int_\Omega e_\varepsilon^{(\kappa)}(\rho,\mathbf{v},\mathbf{w})\,\mathrm{d}\mathbf{x}$$

where

$$e_\varepsilon^{(\kappa)}(\rho,\mathbf{v},\mathbf{w})=\frac{\rho}{2}\Big(|\mathbf{w}|^2+(\varepsilon^2+4\kappa(1-\kappa)\nu^2)|\mathbf{v}|^2\Big)+\frac{\rho^\gamma}{\gamma-1}+2r\nu\kappa\rho\log\rho, \tag{5.2}$$

it can be proved that there exists $C_{\nu,\kappa}>0$ only depending on ν and κ such that:

$$\frac{\mathrm{d}E_\varepsilon^{(\kappa)}}{\mathrm{d}t}(\rho,\mathbf{v},\mathbf{w})+C_{\nu,\kappa}\Big[\int_\Omega\gamma\rho^{\gamma-2}|\nabla\rho|^2\,\mathrm{d}\mathbf{x}+\varepsilon^2\int_\Omega\rho|\nabla\mathbf{v}|^2\,\mathrm{d}\mathbf{x}+\int_\Omega\rho|\nabla\mathbf{u}|^2\mathrm{d}\mathbf{x}\Big]+r\int_\Omega\rho|\mathbf{u}|^2\,\mathrm{d}\mathbf{x}\le 0. \tag{5.3}$$

The inequality (5.3) is available in [8]: see (6) given in the Definition 2, using $p(\rho)=\rho^\gamma$, $\mu(\rho)=\nu\rho$, $\lambda(\rho)=0$ and $K(\rho)=1/\rho$. Unfortunately, the constant $C_{\nu,\kappa}$ is no more explicit, and the proof of Lemma 2.1 is no more valid. Indeed, instead of $\nu\,\mathrm{div}(\rho\nabla\mathbf{w})$ arising in the right-hand-side of (2.1b) in the case $\kappa=1/2$, we have the more general formulation $2\nu\Big[\mathrm{div}(\rho D(\mathbf{w})-\kappa\,\mathrm{div}(\rho\nabla^T\mathbf{w})\Big]$ in the right-hand-side of (5.1b) and the sign of $\nu(1-2\kappa)\int_\Omega\mathrm{div}(\rho\nabla^T\mathbf{w})\cdot\mathbf{w}\mathrm{d}\mathbf{x}$ can not be controlled. Nevertheless, in the particular case $d=1$, system (5.1) becomes:

$$\partial_t\widetilde{U}+\partial_x\widetilde{F}(\widetilde{U})=\partial_x\widetilde{M}(\widetilde{U})+\widetilde{S}(\widetilde{U}), \tag{5.4}$$

where

$$\widetilde{U}=\begin{bmatrix}\rho\\ \rho w\\ \rho v\end{bmatrix},\quad \widetilde{F}(\widetilde{U})=\begin{bmatrix}\rho w\\ \rho w^2+p(\rho)+2r\kappa\nu\rho\\ \rho vw\end{bmatrix},\quad \widetilde{S}(\widetilde{U})=\begin{bmatrix}0\\ -r\rho w+4r\kappa\nu\partial_x\rho\\ 0\end{bmatrix},$$

and

$$\widetilde{M}(\widetilde{U})=\begin{bmatrix}2\kappa\nu\partial_x\rho\\ 2\kappa\nu w\partial_x\rho+(\varepsilon^2-4\kappa(1-\kappa)\nu^2)\rho\partial_x v+2(1-\kappa)\nu\rho\partial_x w\\ 2\kappa\nu v\partial_x\rho-\rho\partial_x w+2\kappa\nu\rho\partial_x v\end{bmatrix}.$$

Consequently, it is easy to check that the proof of Lemma 2.1 can be adapted to the case $\kappa\in(0,1)$ since for any function from $\mathbb{R}$ in $\mathbb{R}$, the ∇ and ∇^Toperators both reduce to the ∂_x one, so that the following result can be proved:

Corollary 5.1. *Suppose that (ρ,v,w) is a strong enough solution of (5.4) and $\Omega=(a,b)$. We further define $u=w-2\kappa\nu v$. Then, for any $\kappa\in(0,1)$ we have:*

$$\frac{\mathrm{d}E_\varepsilon^{(\kappa)}}{\mathrm{d}t}(\rho,v,w)+\int_a^b\left(2\kappa\nu\gamma\rho^{\gamma-2}(\partial_x\rho)^2+2\kappa\nu\varepsilon^2\rho(\partial_x v)^2+2(1-\kappa)\nu\rho(\partial_x u)^2+r\rho u^2\right)\mathrm{d}x=0. \tag{5.5}$$

Defining now the discrete κ-entropy at time t_n as

$$E_\varepsilon^{(\kappa,dis)}(\widetilde{U}^n)=h_1\sum_{i=1}^{N_1}e_\varepsilon^{(\kappa)}(\widetilde{U}_i^n), \tag{5.6}$$

and proceeding in the same manner as in the proof of Theorem 4.4, we can easily show the discrete counterpart of (5.5).

Corollary 5.2. *Suppose that $\widetilde{U}^{n+\frac12}$ and $\widetilde{U}^{n+1}$ are computed in 1D in the same manner as in the 2D scheme developed in Section 3, and that the κ-entropy $E_\varepsilon^{(\kappa,dis)}(\widetilde{U}^n)$ is now defined by (5.6). Then we have:*

$$E_\varepsilon^{(\kappa,dis)}(\widetilde{U}^{n+1})+\Delta t(\widetilde{T}_p(\widetilde{U}^{n+1})+\widetilde{T}_v(\widetilde{U}^{n+1})+\widetilde{T}_u(\widetilde{U}^{n+1})+\widetilde{T}_r(\widetilde{U}^{n+1}))\le E_\varepsilon^{(\kappa,dis)}(\widetilde{U}^n) \tag{5.7}$$

where:

$$\widetilde{T}_p(\widetilde{U}) = 2\kappa\nu\gamma h_1 \sum_i \widetilde{\rho}_{i-\frac{1}{2}}^{\gamma-2} \left(\frac{(\delta_1\rho)_{i-\frac{1}{2}}}{h_1} \right)^2,$$

$$\widetilde{T}_v(\widetilde{U}) = 2\kappa\nu\varepsilon^2 h_1 \sum_i \rho_{i-\frac{1}{2}} \left(\frac{(\delta_1 v)_{i-\frac{1}{2}}}{h_1} \right)^2,$$

$$\widetilde{T}_u(\widetilde{U}) = 2(1-\kappa)\nu h_1 \sum_i \rho_{i-\frac{1}{2}} \left(\frac{(\delta_1 w)_{i-\frac{1}{2}}}{h_1} - 2\kappa\nu \frac{(\delta_1 v)_{i-\frac{1}{2}}}{h_1} \right)^2,$$

$$\widetilde{T}_r(\widetilde{U}) = r h_1 \sum_i \rho_i \left(w_i - \frac{2\kappa\nu(\delta_1\rho)_{i-\frac{1}{2}}}{h_1 \sqrt{\rho_i \widehat{\rho}_{i-\frac{1}{2}}}} \right)^2.$$

6. **Numerical tests**

6.1. **1D-benchmarks**

6.1.1. *The one-dimensional "gray" soliton*

In order to verify the efficiency of the scheme, we aim to reproduce results presented in [13], starting from the nonlinear Schrödinger equation :

$$i\partial_t\Psi + \frac{1}{2}\Delta\Psi - f(|\Psi|^2)\Psi = 0, \tag{6.1}$$

where f is a function of $|\Psi|^2$ caracterizing the nonlinearity of the equation. It can be rewritten in an hydrodynamic formulation using the Madelung's transform [25, 28], which corresponds to the system (1.1a)–(1.1b) in the case $f(\rho) = \rho$, $\varepsilon = 1/2$, $\nu = r = 0$ and $p(\rho) = \rho^2/2$. Then, by looking for traveling wave solutions in the form:

$$\rho(t,x) = \rho(\zeta), \quad u(t,x) = u(\zeta) \quad \text{with } \zeta = x - Ut \text{ and } U \in \mathbb{R},$$

it can be shown that a family of analytical solutions, called "gray" solitons, is defined by

$$\rho(t,x) = b_1 - \frac{b_1 - b_3}{\cosh^2(\sqrt{b_1 - b_3}(x - Ut))} \quad \text{and} \quad u(t,x) = U - \frac{b_1\sqrt{b_3}}{\rho(t,x)}. \tag{6.2}$$

Consequently, the analytical solution of system (5.4) with $\varepsilon = 1/2$, $\nu = r = 0$ and $p(\rho) = \rho^2/2$ is given by (6.2) as well as :

$$w(t,x) = u(t,x) \quad \text{and} \quad v(t,x) = \partial_x \log\rho(t,x).$$

Figure 6.1 (A) (respectively, Figure 6.2 (A)) shows the value of ρ_h (respectively, u_h) in the domain $\Omega = (-20, 20)$ for $b_1 = 1.5$, $b_3 = 1$ and $U = 2$, at time $t = 40$ which corresponds to two full periods, and for several values of N_1 ranging from $N_1 = 10^4$ to $N_1 = 2.10^5$. Moreover, the L_2-norm of the errors in ρ, u and v between the numerical and exact solutions is shown in Table 6.1. As we can see, the numerical solution converges to the exact one with an order equal to one as the mesh is refined. We also calculate the value of v_r in post-processing, an approximation of v recalculated from the discrete gradient of $log\rho_h$, in order to highlight the convergence of v_h towards v_r. We observe a convergence of order one (see the last column in the Table 6.1) which also implies, by the triangular inequality, the convergence of v_r towards v. The evolution of the BD-entropy over time is shown in Figure 6.2 (B) for the same values of N_1 (the definition (5.2) of $e_\varepsilon^{(\kappa)}$ is therefore modified by replacing $\rho^\gamma/(\gamma-1)$ with $\rho^2/2$, since $p(\rho) = \rho^2/2$). It is observed that the larger N_1, the smaller the decrease in BD-entropy,

which is the expected behavior since in this configuration the BD-entropy is conserved (see (1.8) with $\nu = r = 0$).

Remark 6.1. From a theoretical point of view, we could expect a convergence rate equal to one, due to the use of the Rusanov scheme in the hyperbolic step, which is actually first-order accurate. It should be noted that the order of convergence could be improved by using a second-order flux reconstruction with slope limiters in the hyperbolic part. However, to the best of our knowledge, such an approach would prevent the derivation of Lemma 4.1, and consequently, of Theorem 4.4.

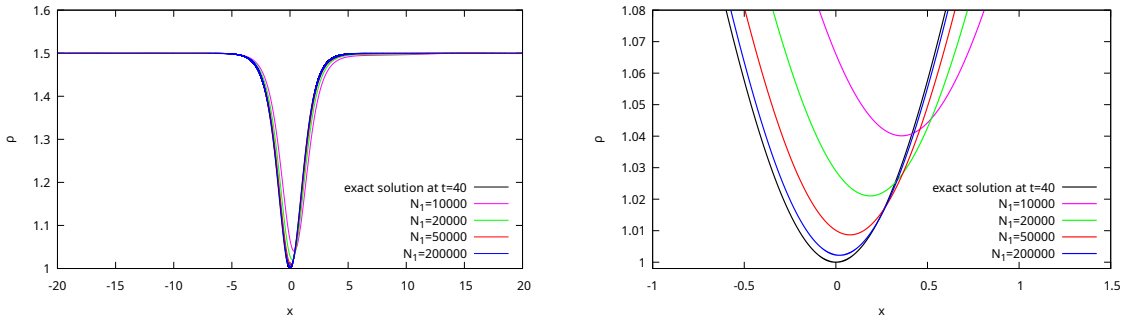

(A) ρ at $t = 40$. (B) zoom of Figure 6.1 (A) in the vicinity of $x = 0$.

FIGURE 6.1. The "gray" soliton : density.

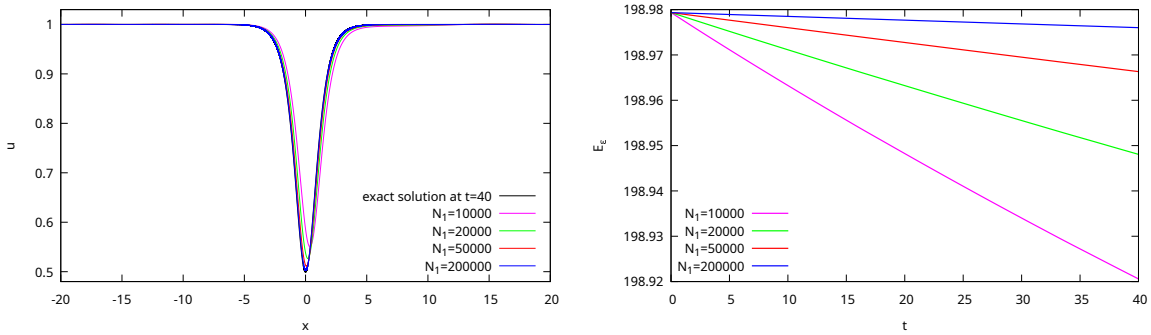

(A) u at $t = 40$. (B) BD-entropy over time.

FIGURE 6.2. The "gray" soliton : velocity and BD-entropy decay.

N_1	$\|\rho_h - \rho\|$	order	$\|u_h - u\|$	order	$\|v_h - v\|$	order	$\|v_h - v_r\|$	order
10000	0.1559		0.1633		0.0803		5.3326×10^{-4}	
20000	0.0836	0.90	0.0884	0.89	0.0442	0.86	2.7191×10^{-4}	0.97
50000	0.0349	0.95	0.0371	0.95	0.0187	0.94	1.0952×10^{-4}	0.99
200000	0.0089	0.98	0.0095	0.98	0.0048	0.98	2.7397×10^{-5}	1.00

TABLE 6.1. L^2-Errors and convergence orders for different mesh refinements at $t = 40$.

6.1.2. *The dispersive Riemann problem*

The second 1D-benchmark consists in the propagation of a dispersive shock wave, characterized by the appearance of an oscillatory wave train in a region of space which expands over time (see e.g. [16, 17, 18]), which is also solution of system (5.4) with $\varepsilon = 1/2$ $\nu = r = 0$, and $p(\rho) = \rho^2/2$. As in the previous benchmark, the definition (5.2) of $e_\varepsilon^{(\kappa)}$ is modified accordingly, replacing $\rho^\gamma/(\gamma-1)$ with $\rho^2/2$. The amplitude of this dispersive shock wave is described by Whitham's modulation equations [33]. Considering the parameters ρ_L, ρ_R, u_L and u_R, as well as a regularization parameter $\delta > 0$, the initial solution is defined by:

$$\rho_0(x) = \rho_M - \left(\frac{\rho_L - \rho_R}{2}\right)\tanh\left(\frac{x}{\delta}\right), \quad u_0(x) = u_M - \left(\frac{u_L - u_R}{2}\right)\tanh\left(\frac{x}{\delta}\right),$$

with $\rho_M = (\rho_L + \rho_R)/2$ and $u_M = (u_L + u_R)/2$. It can be shown that the asymptotic profile of the solution is characterized by the parameters τ_i $(1 \leq i \leq 4)$ delimiting the different regions of the solution expressed as a function of $\tau = x/t$, like displayed in Figure 6.3 (coming from [13, Figure 2]), and given by:

$$\tau_1 = u_R + \frac{8\rho_M - 8\sqrt{\rho_M\rho_R} + \rho_R}{2\sqrt{\rho_M} - \sqrt{\rho_R}}, \quad \tau_2 = u_R + \sqrt{\rho_M}, \quad \tau_3 = u_M - \sqrt{\rho_M} \quad \text{and} \quad \tau_4 = u_L - \sqrt{\rho_L}.$$

Let us remark that the oscillatory profile occurs between τ_2 and τ_1.

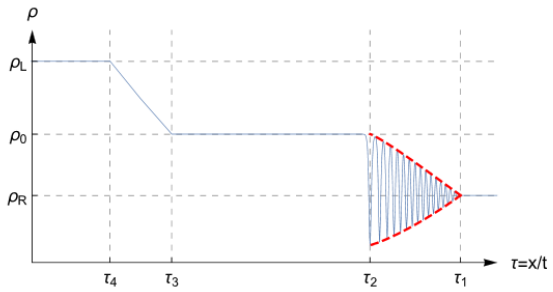

Figure 6.3. Asymptotic profile of the density ρ for the dispersive Riemann Problem.

Numerical tests are performed using $\rho_L = 2$, $\rho_R = 1$, $u_L = u_R = 0$ and $\delta = 0.1$. The density profile is displayed in Figure 6.4 at several times, to observe the evolution towards the stationary state. Moreover, the density and velocity profiles at time $t = 70$ are displayed in Figure 6.5. From a qualitative point of view, the wave train evolves towards its stationary state. At $t = 70$, the asymptotic profile is close to the expected Witham envelope, like obtained in [13].

We then provide more quantitative indicators. On the one hand, we investigate the convergence of the numerical solution of system (2.1) towards a reference solution of the initial barotropic QNS system (1.1). To do this, system (1.1) is solved using a time-implicit centered finite difference scheme on staggered grids used in [19, Section 5] in the context of a numerical simulation of a resonant tunneling diode. The mesh is composed of 1.6×10^6 cells, which allows us to obtain a sufficiently accurate reference solution (ρ_{ref}, u_{ref}). Table 6.2 shows the convergence obtained in ρ and u at time $t = 14$. We observe that the numerical solutions of system (2.1) converge to the reference one of system (1.1) when the mesh is refined.

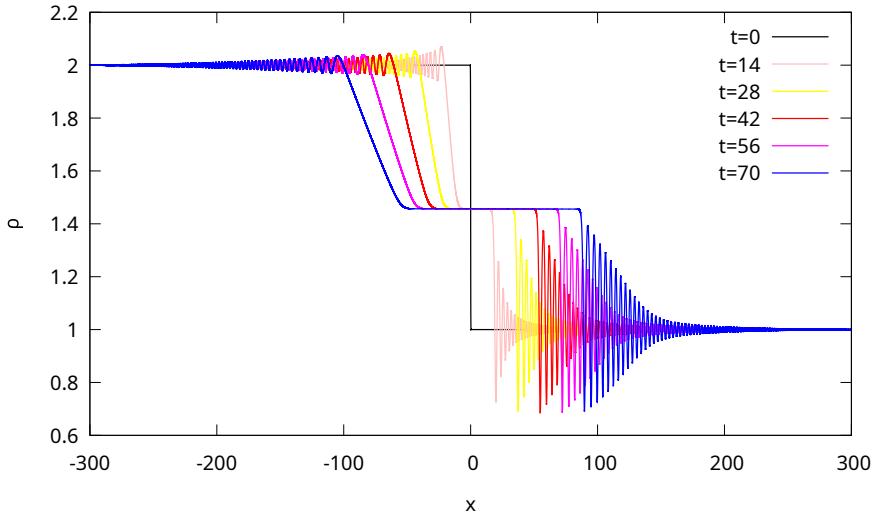

FIGURE 6.4. Density ρ for different times, $\Omega = (-300, 300)$, $N_1 = 400000$.

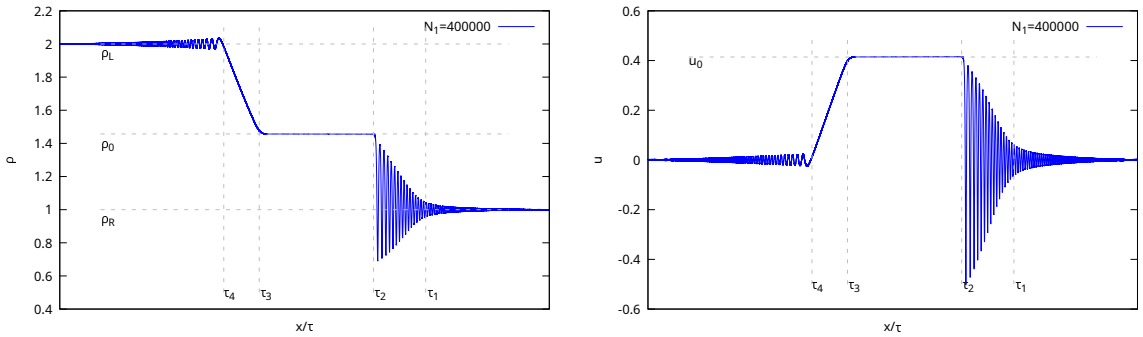

(A) ρ at $t = 70$.

(B) u at $t = 70$.

FIGURE 6.5. Solution (ρ, u) at $t = 70$, $\Omega = (-300, 300)$, $N_1 = 400000$.

N_1	$\|\rho_h - \rho_{ref}\|$	$\|u_h - u_{ref}\|$
25000	0.2714	0.3903
50000	0.1865	0.2853
100000	0.1145	0.1860
200000	0.0612	0.1079
400000	0.0209	0.0383

TABLE 6.2. L^2-errors in ρ and u with a reference solution of the original QNS system at $t = 14$.

On the other hand, we investigate the long time behavior of the solution. A simulation is done using up to $t = 200$. In Figure 6.6 (A), we display the value of $at^{3/2}$ as a function of t, where a corresponds to the amplitude of the first oscillation on the left vicinity of τ_4. Since it corresponds to a linear function, it implies that $a\sqrt{t}$ is constant in time, so that the amplitudes decrease in time in $O(1/\sqrt{t})$, as physically expected (see [22]). We are also interested in the position of the soliton at the vicinity of

$\tau = \tau_2$. By denoting $\tau_s(t)$ the soliton position at time t, we plot in Figure 6.6 (B) the value of $err_{pos}(t)$ as a function of the time, where $err_{pos}(t)$ is defined by:

$$err_{pos}(t) = \left| \frac{\tau_s(t) - \tau_2}{\tau_2} \right|.$$

Once again, it can be seen that this result is similar to the one otained in [13].

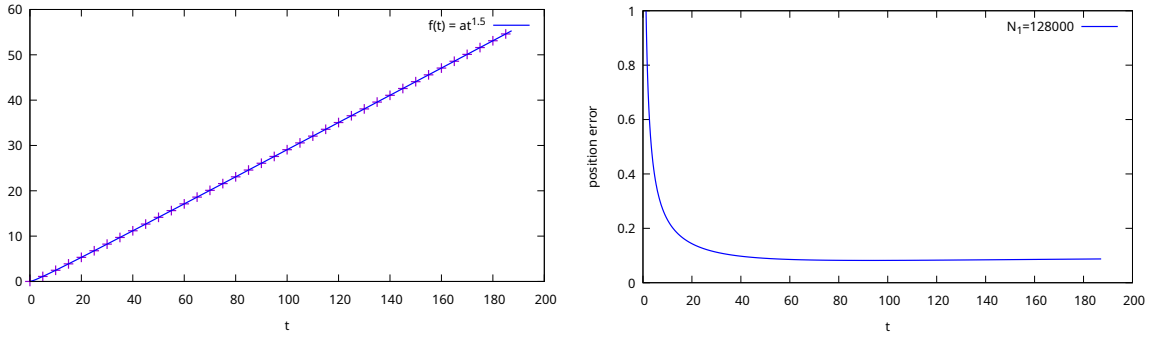

(A) $at^{3/2}$ versus t. (B) $err_{pos}(t)$ versus t.

FIGURE 6.6. Long time behavior of the solution, $\Omega = (-400, 400)$, $N_1 = 128000$.

Finally, we investigate the solution profile when ν is no longer equal to zero, taking $\kappa = 1/2$. Figure 6.7 displays the value of ρ at time $t = 70$ for different values of ν (with a zoom at the bottom left between $x = 80$ and $x = 150$). In order to observe the numerical decreasing behavior of κ-entropy, we also introduce the quantity $E_\varepsilon^{(\kappa,dis,th)}(\widetilde{U}^n)$ defined from $E_\varepsilon^{(\kappa,dis)}(\widetilde{U}^0)$ (see (5.6)) by:

$$\begin{cases} E_\varepsilon^{(\kappa,dis,th)}(\widetilde{U}^0) = E_\varepsilon^{(\kappa,dis)}(\widetilde{U}^0), \\ E_\varepsilon^{(\kappa,dis,th)}(\widetilde{U}^{n+1}) = E_\varepsilon^{(\kappa,dis,th)}(\widetilde{U}^n) - \Delta t(\widetilde{T}_p(\widetilde{U}^{n+1}) + \widetilde{T}_v(\widetilde{U}^{n+1}) + \widetilde{T}_u(\widetilde{U}^{n+1}) + \widetilde{T}_r(\widetilde{U}^{n+1})). \end{cases}$$

From (5.7), it is clear that

$$\forall\, n \in \mathbb{N}, \quad E_\varepsilon^{(\kappa,dis)}(\widetilde{U}^n) \leq E_\varepsilon^{(\kappa,dis,th)}(\widetilde{U}^n). \tag{6.3}$$

Figure 6.8 (A) shows the values of $E_\varepsilon^{(1/2,dis)}$ (solid lines) and of $E_\varepsilon^{(1/2,dis,th)}$ (dashed lines) as a function of time for several values of ν. We can see that the larger ν is, the more regular the profile is, and the greater the decrease in BD-entropy. Moreover, for a given value of ν, we can see that as expected by the relation (6.3), that the value of $E^{(\kappa,dis)}$ is always smaller than the value of $E^{(\kappa,dis,th)}$. In the particular case $\nu = 0$ (and $r = 0$), the value of $E^{(\kappa,dis,th)}$ is constant, and the decrease of $E^{(\kappa,dis)}$ is solely due to the numerical diffusion, both in the hyperbolic step and in the parabolic one.

Finally, we plot in Figure 6.8 (B) the discrete version of the energy $\mathcal{E}_\varepsilon$ given by (1.2) (replacing $\rho^\gamma/(\gamma-1)$ by $\rho^2/2$ since $p(\rho) = \rho^2/2$), in order to emphasize that, as predicted theoretically from (1.3), the energy decreases with time, and the greater the value of ν, the faster it tends towards zero.

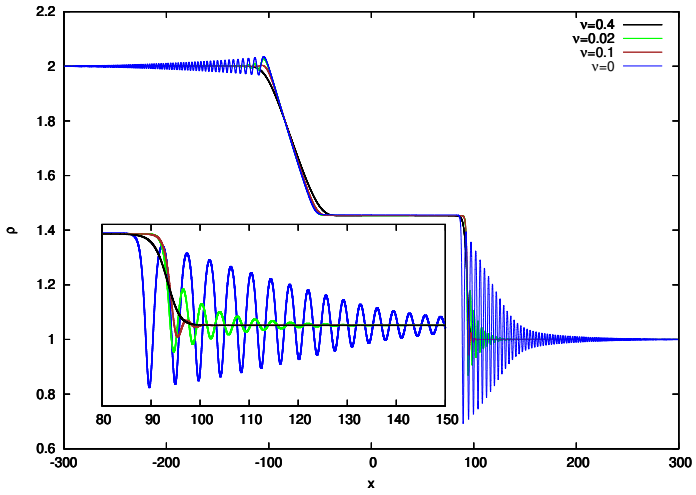

FIGURE 6.7. ρ at $t = 70$ for different values of ν.

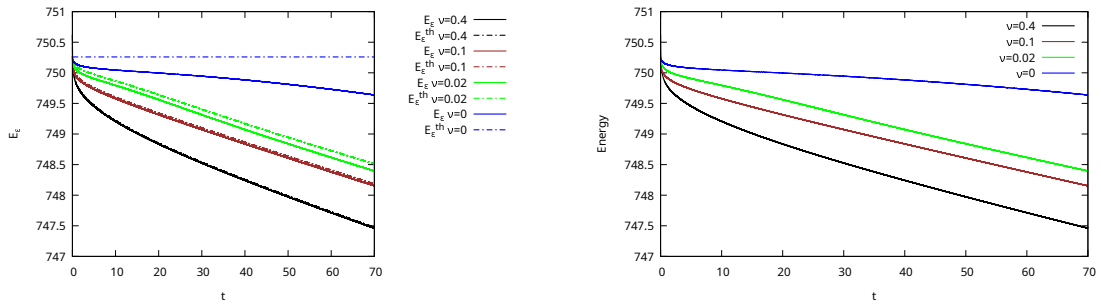

(A) BD-entropy versus t for different values of ν. (B) Energy versus t for different values of ν.

FIGURE 6.8. BD-entropy and energy versus t for different values of ν. $\Omega = (-300, 300)$, $N_1 = 400000$.

6.2. **2D-benchmark**

We finally propose here a 2D-benchmark in order to illustrate the convergence of the numerical scheme. To our best knowledge, there is no analytical solution available for the QNS system (1.1) in the 2D case. Consequently, we consider the following periodic density and velocity field given for $c > 0$ and $\sigma > 0$ on $\Omega = [-L, L]^2$ (with $L = 10$) by:

$$\rho(t, \mathbf{x}) = 1 + e^{-r^2(t,\mathbf{x})} \text{ and } \mathbf{u}(t, \mathbf{x}) = \left(\cos\left(\frac{\pi}{L}x_1\right),\ \sin\left(\frac{\pi}{L}x_2\right)\right)^T, \tag{6.4}$$

where

$$r^2(t, \mathbf{x}) = \frac{(x_1 - ct)^2 + x_2^2}{2\sigma}.$$

We add source terms to the equations (2.1a), (2.1b) and (2.1c), so that $(\rho, \mathbf{w}, \mathbf{v})$ constitutes a solution of the system, where $\mathbf{v}$ and $\mathbf{w}$ verify (1.4) and (1.5). Having set $c = 10$ and $\sigma = 3.6$, the initial condition is shown in Figure 6.9. The physical parameters are given by $\varepsilon = 1$, $\nu = \frac{1}{2}$ and the numerical simulation is performed up to $t = 2$, which corresponds to exactly one period for the exact solution.

We study the convergence rate of the method in order to evaluate how close the numerical solution is to the analytical one. Table 6.3 shows the L^2-norm of the errors in ρ, $\mathbf{w}$ and $\mathbf{v}$ for values of $N_1 = N_2$

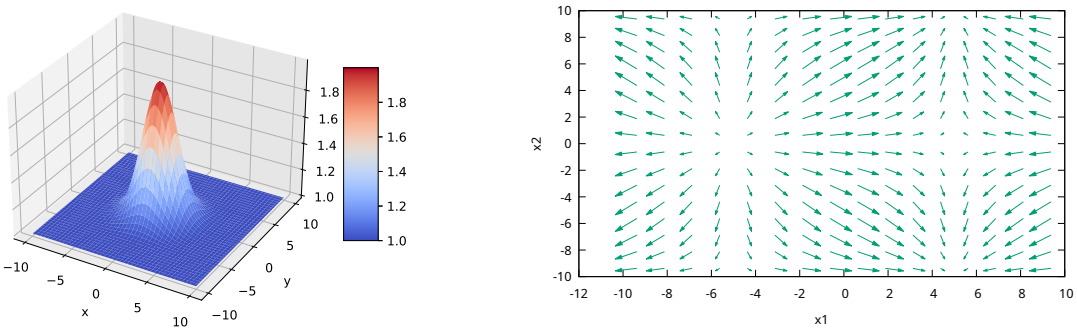

(A) $\rho(0,\mathbf{x})$ (B) $\mathbf{u}(0,\mathbf{x})$

Figure 6.9. 2D-benchmark : Initial condition.

between 32 and 512. As expected theoretically, the scheme is first-order accurate in both space and time. Table 6.4 also shows the convergence rate of some post processing calculated values. First we observe that the reconstructed velocity $\mathbf{u}_r = \mathbf{w}_h - \nu \mathbf{v}_h$ converges to $\mathbf{u}$ at order one. Next, similarly to what was done in Subsection 6.1.1, the value of $\mathbf{v}_r$, defined as the discrete gradient of $\log \rho_h$, converges asymptotically to $\mathbf{v}_h$ at order one. This also implies, by the triangular inequality, that $\mathbf{v}_h$ converges to $\mathbf{v}$ to the same order. We also compute $\nabla_h \times \mathbf{v}_h$, defined as the discrete curl of $\mathbf{v}_h$, to emphasize that the value of $\|\nabla_h \times \mathbf{v}_h\|$ converges to zero at order one. Finally, we illustrate the fact that $|\nabla_h \times \mathbf{v}_h|$ as well as $\left|\|\mathbf{v}_h\|_2 - \|\mathbf{v}_r\|_2\right|$ tend towards zero in the infinite norm (see the isovalues of these quantities for three mesh refinements respectively in Figures 6.10 and 6.11).

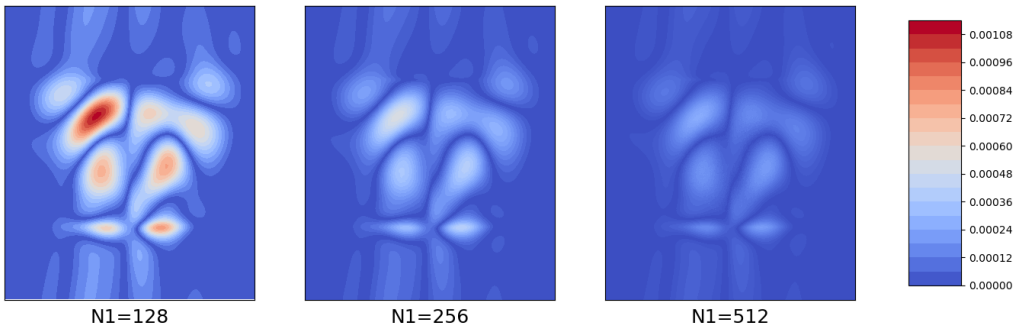

Figure 6.10. 2D-benchmark : Isovalues of $|\nabla_h \times \mathbf{v}_h|$ for three mesh refinements.

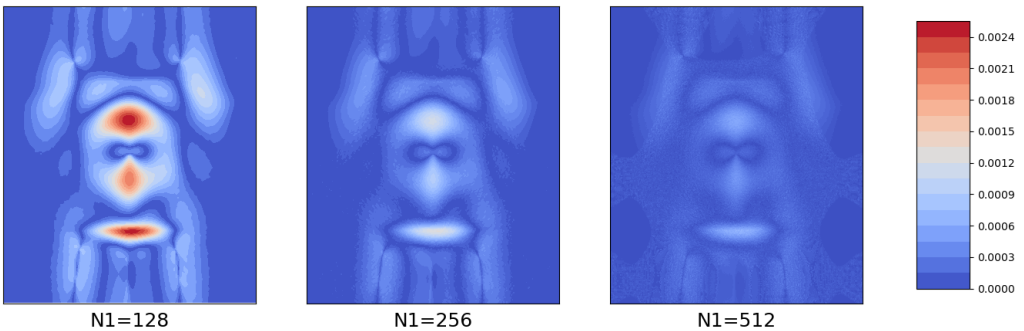

Figure 6.11. 2D-benchmark : Isovalues of $\left|\|\mathbf{v}_h\|_2 - \|\mathbf{v}_r\|_2\right|$ for three mesh refinements.

N_1	$\|\rho_h - \rho\|$	order	$\|\mathbf{w}_h - \mathbf{w}\|$	order	$\|\mathbf{v}_h - \mathbf{v}\|$	order
32	0.6791		0.9909		0.3359	
64	0.3384	1.00	0.5141	0.95	0.1722	0.96
128	0.1692	1.00	0.2620	0.97	0.0870	0.98
256	0.0846	1.00	0.1324	0.99	0.0436	1.00
512	0.0422	1.00	0.0665	0.99	0.0216	1.00

TABLE 6.3. L^2-Errors and convergence orders for different mesh refinements at $t = 2$.

N_1	$\|\mathbf{u}_r - \mathbf{u}\|$	order	$\|\mathbf{v}_r - \mathbf{v}_h\|$	order	$\|\nabla_h \times \mathbf{v}_h\|$	order
32	0.9279	0.88	0.0717	1.65	0.0198	1.34
64	0.4834	0.94	0.0272	1.39	0.0094	1.06
128	0.2471	0.97	0.0120	1.17	0.0045	1.05
256	0.1250	0.98	0.0058	1.05	0.0022	1.03
512	0.0628	0.99	0.0030	0.92	0.0011	1.03

TABLE 6.4. Post processing calculated values behavior at $t = 2$.

7. Concluding remarks and perspectives

In this paper, we propose a Finite Volume scheme that preserves the so-called Bresch–Desjardins entropy inequality for the approximation of the Quantum Navier–Stokes system. The method is based on a reformulation of the original system into an augmented one in $(\rho, \mathbf{w}, \mathbf{v})$, defined respectively as density, effective velocity and drift velocity. This work can be understood in the spirit of that developed in [2, 3], in which an energy inequality was derived using the system expressed in the variables $(\rho, \mathbf{u}, \mathbf{v})$. A splitting in time allows us to consider first the hyperbolic step which can be handled with a standard Finite-Volume solver, and then the parabolic step, which in our configuration remains linear. Thanks to a particular discretization of some of the differential operators involved, it has been proved that the BD-entropy also decreases in the discrete case. The proposed scheme has been validated on several benchmarks. It shows a good ability to capture physical behaviors on well-known configurations such as the one-dimensional "gray" soliton or the dispersive Riemann problem. It also demonstrates its ability to converge to some analytical solutions that have been constructed or reference solutions that have been computed directly from the original Quantum Navier–Stokes system. We are now considering adapting this method to obtain finite volume schemes that preserve entropy inequalities for more general models, such as for example Navier–Stokes Korteweg systems modeling some multiphase flows or shallow-water systems modeling thin film flows with several kind of capillary values. Another point to be investigate is to increase the order of accuracy of the method in space, while preserving the discrete BD-entropy inequality.

Acknowledgments

The authors would like to thank Ingrid Lacroix-Violet and Jean-Claude Magnier for fruitful discussions about this work.

Appendix A. Proof of the consistency of (3.10) and (3.11)

Let us consider $\alpha : \mathbb{R}^2 \to \mathbb{R}$ and $\beta : \mathbb{R}^2 \to \mathbb{R}$ as regularly as necessary. We define :

$$\bar{\alpha}_{i,j} = \alpha((x_1)_i, (x_2)_j) \text{ and } \bar{\beta}_{i,j} = \beta((x_1)_i, (x_2)_j).$$

Then we have:

$$\sqrt{\bar{\alpha}_{i-\frac{1}{2},j+1}\bar{\alpha}_{i,j+\frac{1}{2}}} = \bar{\alpha}_{i-\frac{1}{2},j+1} + \mathcal{O}(h_1 + h_2)$$

as well as:

$$\frac{\bar{\beta}_{i,j+1} - \bar{\beta}_{i-1,j+1}}{h_1} = (\partial_1\bar{\beta})_{i-\frac{1}{2},j+1} + \mathcal{O}(h_1^2),$$

so that:

$$\frac{\sqrt{\bar{\alpha}_{i-\frac{1}{2},j+1}\bar{\alpha}_{i,j+\frac{1}{2}}}(\bar{\beta}_{i,j+1} - \bar{\beta}_{i-1,j+1})}{h_1} = \bar{\alpha}_{i-\frac{1}{2},j+1}(\partial_1\bar{\beta})_{i-\frac{1}{2},j+1} + (\partial_1\bar{\beta})_{i-\frac{1}{2},j+1}\mathcal{O}(h_1 + h_2) + \bar{\alpha}_{i-\frac{1}{2},j+1}\mathcal{O}(h_1^2) + \mathcal{O}(h_1^3 + h_1^2 h_2). \quad \text{(A.1)}$$

Similarly, we have:

$$\frac{\sqrt{\bar{\alpha}_{i-\frac{1}{2},j}\bar{\alpha}_{i,j-\frac{1}{2}}}(\bar{\beta}_{i,j} - \bar{\beta}_{i-1,j})}{h_1} = \bar{\alpha}_{i-\frac{1}{2},j}(\partial_1\bar{\beta})_{i-\frac{1}{2},j} + (\partial_1\bar{\beta})_{i-\frac{1}{2},j}\mathcal{O}(h_1 + h_2) + \bar{\alpha}_{i-\frac{1}{2},j}\mathcal{O}(h_1^2) + \mathcal{O}(h_1^3 + h_1^2 h_2). \quad \text{(A.2)}$$

Consequently,

$$\begin{aligned}
&\frac{\sqrt{\bar{\alpha}_{i-\frac{1}{2},j+1}\bar{\alpha}_{i,j+\frac{1}{2}}}(\bar{\beta}_{i,j+1} - \bar{\beta}_{i-1,j+1}) - \sqrt{\bar{\alpha}_{i-\frac{1}{2},j}\bar{\alpha}_{i,j-\frac{1}{2}}}(\bar{\beta}_{i,j} - \bar{\beta}_{i-1,j})}{h_1 h_2} \\
&\quad = \frac{\bar{\alpha}_{i-\frac{1}{2},j+1}(\partial_1\bar{\beta})_{i-\frac{1}{2},j+1} - \bar{\alpha}_{i-\frac{1}{2},j}(\partial_1\bar{\beta})_{i-\frac{1}{2},j}}{h_2} + \frac{(\partial_1\bar{\beta})_{i-\frac{1}{2},j+1} - (\partial_1\bar{\beta})_{i-\frac{1}{2},j}}{h_2}\mathcal{O}(h_1 + h_2) \\
&\qquad + \frac{\bar{\alpha}_{i-\frac{1}{2},j+1} - \bar{\alpha}_{i-\frac{1}{2},j}}{h_2}\mathcal{O}(h_1^2) + \mathcal{O}\left(\frac{h_1^3}{h_2} + h_1^2\right) \\
&\quad = (\partial_2(\bar{\alpha}\partial_1\bar{\beta}))_{i-\frac{1}{2},j+\frac{1}{2}} + \mathcal{O}(h_2^2) + \Big((\partial_2\partial_1\bar{\beta})_{i-\frac{1}{2},j+\frac{1}{2}} + \mathcal{O}(h_2^2)\Big)\mathcal{O}(h_1 + h_2) \\
&\qquad + \Big((\partial_2\bar{\alpha})_{i-\frac{1}{2},j+\frac{1}{2}} + \mathcal{O}(h_2^2)\Big)\mathcal{O}(h_1^2) + \mathcal{O}\left(\frac{h_1^3}{h_2} + h_1^2\right).
\end{aligned}$$

From (3.1), we deduce:

$$\begin{aligned}
\frac{\sqrt{\bar{\alpha}_{i-\frac{1}{2},j+1}\bar{\alpha}_{i,j+\frac{1}{2}}}(\bar{\beta}_{i,j+1} - \bar{\beta}_{i-1,j+1}) - \sqrt{\bar{\alpha}_{i-\frac{1}{2},j}\bar{\alpha}_{i,j-\frac{1}{2}}}(\bar{\beta}_{i,j} - \bar{\beta}_{i-1,j})}{h_1 h_2} &= (\partial_2(\bar{\alpha}\partial_1\bar{\beta}))_{i,j} + \mathcal{O}(h(1 + \tau h)), \\
&= (\partial_2(\bar{\alpha}\partial_1\bar{\beta}))_{i,j} + \mathcal{O}(h)
\end{aligned}$$

since τ is uniformly bounded. Consequently, (3.10) corresponds to a discretization of the continuous operator at point $X_{i,j}$ to order one in each direction. We proceed similarly for (3.11).

Appendix B. Study of the $Sp(M)$ in the case $\varepsilon > \nu > 0$

Suppose that the unknowns are enumerated from the left to the right ($1 \leq i \leq N_1$) and from the bottom to the top ($1 \leq j \leq N_2$). Denoting $\bar{U}_h^{n+1}$ the vector $\bar{U}_h^{n+1} = [(\rho w_1)_{i,j}, (\rho w_2)_{i,j}, (\rho v_1)_{i,j}, (\rho v_2)_{i,j}]^T$, the linear system (3.20) takes the form

$$\bar{U}_h^{n+1} = M\bar{U}_h^{n+\frac{1}{2}} + 2r\nu \begin{bmatrix} (\partial_1\rho)_{i,j}^{n+1} \\ (\partial_2\rho)_{i,j}^{n+1} \\ 0 \\ 0 \end{bmatrix}$$

with

$$M = I_{4N_1N_2} + \Delta t C \ \in \mathcal{M}_{4N_1N_2}(\mathbb{R})$$

where $C = C^{(1)} + C^{(2)}$ with

$$C^{(1)} = \begin{pmatrix} rI_{N_1N_2} & 0 & \varepsilon^2 C_{13} & \varepsilon^2 C_{14} \\ 0 & rI_{N_1N_2} & \varepsilon^2 C_{23} & \varepsilon^2 C_{24} \\ -\varepsilon^2 C_{13} & -\varepsilon^2 C_{14} & 0 & 0 \\ -\varepsilon^2 C_{23} & -\varepsilon^2 C_{24} & 0 & 0 \end{pmatrix} \quad \text{and} \quad C^{(2)} = \begin{pmatrix} \nu C_0 & 0 & -\nu^2 C_{13} & -\nu^2 C_{14} \\ 0 & \nu C_0 & -\nu^2 C_{23} & -\nu^2 C_{24} \\ 0 & 0 & \nu C_0 & 0 \\ 0 & 0 & 0 & \nu C_0 \end{pmatrix}.$$

Here, $C_0 \in \mathcal{M}_{N_1N_2}(\mathbb{R})$. The matrices C_{13}, C_{14}, C_{23} and C_{24} also belong to $\mathcal{M}_{N_1N_2}(\mathbb{R})$, and only depend on the values of $\rho_{i,j}^{n+1}$.

- In the case $\nu = 0$, which corresponds to $C = C^{(1)}$, it can be easily shown that C is similar to an anti-symmetric matrix. Indeed, denoting $P \in \mathcal{M}_{N_1N_2}(\mathbb{R})$ the diagonal matrix whose diagonal is composed of the coefficients $\sqrt{\rho_{i,j}^{n+1}}$ and $\mathbb{P} \in \mathcal{M}_{4N_1N_2}(\mathbb{R})$ the diagonal matrix defined by

$$\mathbb{P} = \begin{pmatrix} P & 0 & 0 & 0 \\ 0 & P & 0 & 0 \\ 0 & 0 & P & 0 \\ 0 & 0 & 0 & P \end{pmatrix},$$

  we can observe that $P^{-1}C_{13}P$ and $P^{-1}C_{24}P$ are symmetric matrices. Moreover, from the definitions (3.6) and (3.7) we can remark that $\widetilde{\rho}_{i+1,j-\frac{1}{2}} = \widetilde{\rho}_{i+\frac{1}{2},j}$. Consequently, it can be shown that $P^{-1}C_{14}P = (P^{-1}C_{23}P)^T$, so that $\mathbb{P}^{-1}C^{(1)}\mathbb{P} = \mathbb{P}^{-1}C\mathbb{P}$ is an anti-symmetric matrix. We can deduce that

$$Sp(M) \subset \{1 + i\mathbb{R}\},$$

  so M is invertible.

- In the case $\varepsilon > \nu > 0$, C is no more similar to an anti-symmetric matrix. From (3.12), (3.13) and (3.14), it can be shown that :

$$\mathrm{div}(\alpha\nabla\mathbf{a})_{i,j} + \mathrm{div}(\mathbf{a} \otimes \nabla\alpha)_{i,j} = (\Delta(\alpha\mathbf{a}))_{i,j},$$

  so that C_0 is nothing other than the 2-dimensional discrete laplacian operator with periodic boundary conditions. Consequently, C_0 is symmetric and $Sp(C_0) \subset \mathbb{R}^+$. Nevertheless, the question of the invertibility of M does no seem easy to prove. In order to investigate this question, we propose some numerical computations. We set $\Omega =]0, \pi[^2$, $\varepsilon = 1.0$ and $\nu = 0.5$, and we take $N_1 = N_2 = N$. Then, by fixing k_1 modes in x direction and k_2 modes in y

direction, we define the vector $(\rho_{i,j}^{n+1})_{1\leq i,j\leq N} \in (\mathbb{R}_*^+)^{N^2}$ using a random process of the form :

$$\begin{cases} (\rho_{i,j}^{n+1})^P = \displaystyle\sum_{l_1=0}^{k_1-1}\sum_{l_2=0}^{k_2-1} \xi_{1+l_1+k_1 l_2} \sin(l_1(x_1)_i)\sin(l_2(x_2)_j), \\ \rho_{i,j}^{n+1} = \max\left((\rho_{i,j}^{n+1})^P, -\dfrac{(\rho_{i,j}^{n+1})^P}{2}, 10^{-9}\right), \end{cases}$$

where $\zeta \in [-1,1]^{k_1 k_2}$ is a randomly generated vector using a uniform law. Finally, the matrix M is computed using the obtained values of $\rho_{i,j}^{n+1}$. We plot in Figure B.1 the spectrum of M in the complex plane for $N = \{8, 16, 32, 64\}$, each time for a random value of the vector ξ using $k_1 = k_2 = 6$. We observe that in any case and for all $\lambda \in Sp(M)$, $Re(\lambda) \geq 1$. Moreover, it remains always the case whatever the values of ν and ε chosen provided that $\varepsilon > \nu > 0$, whatever the value of $r \geq 0$ and whatever the random value of ξ. Consequenty, we guess that the matrix M il always invertible in the case $\varepsilon > \nu > 0$, even if the theoretical proof remains an open problem.

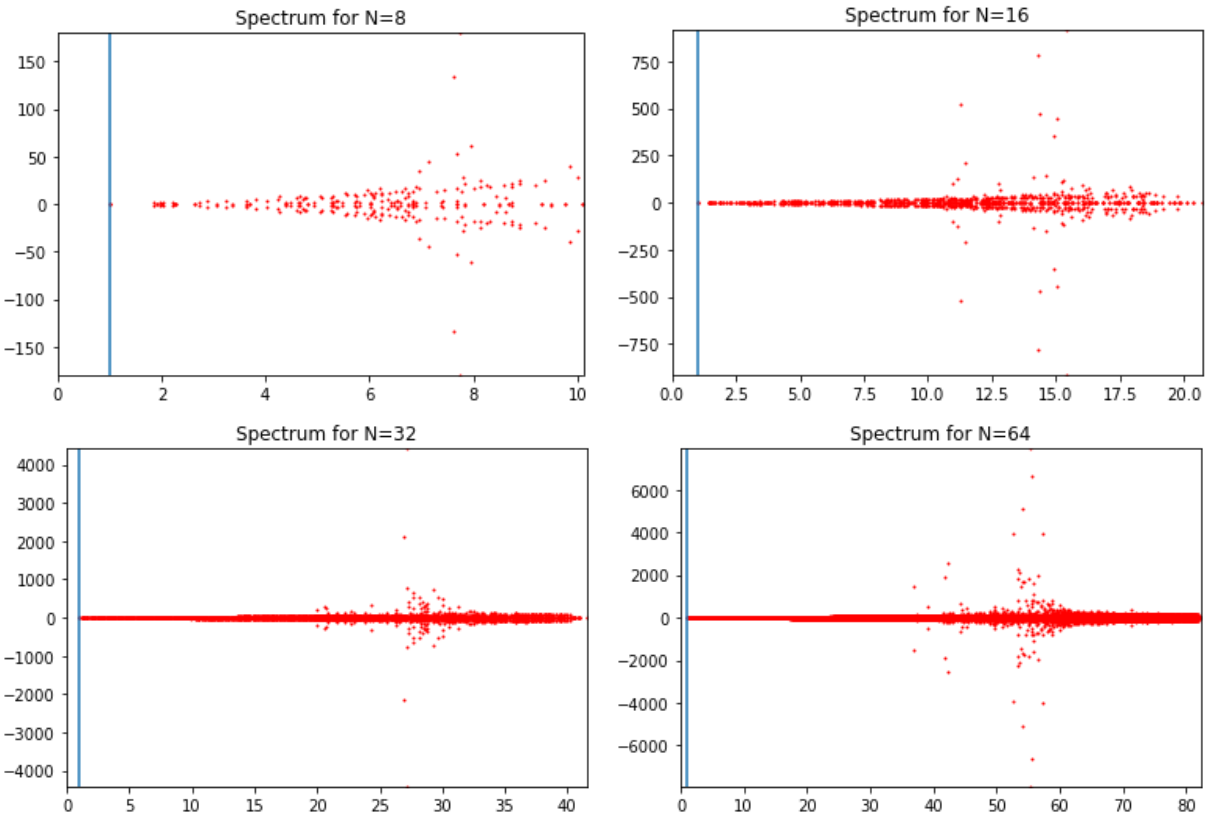

Figure B.1. Spectrum of M for $\varepsilon = 1$, $\nu = 1$, $r = 0$, $\Delta t = h$ and several values of N. In abscissa : real parts. In ordinate : imaginary parts. Vertical blue line : $Re(\lambda) = 1$.

Appendix C. Proof of Lemma 4.2

From (3.15), we get:

$$
\begin{aligned}
&\sum_{i,j} \mathrm{div}(\rho\nabla^T\mathbf{v})_{i,j}\cdot\mathbf{w}_{i,j}\\
&=\sum_{i,j}\Bigg[(w_1)_{i,j}\left(\frac{\rho_{i+\frac12,j}(\delta_1v_1)_{i+\frac12,j}-\rho_{i-\frac12,j}(\delta_1v_1)_{i-\frac12,j}}{h_1^2}+\frac{\sqrt{\rho_{i-\frac12,j+1}\rho_{i,j+\frac12}}(\delta_1v_2)_{i-\frac12,j+1}-\sqrt{\rho_{i-\frac12,j}\rho_{i,j-\frac12}}(\delta_1v_2)_{i-\frac12,j}}{h_1h_2}\right)\\
&\quad+(w_2)_{i,j}\left(\frac{\sqrt{\rho_{i+1,j-\frac12}\rho_{i+\frac12,j}}(\delta_2v_1)_{i+1,j-\frac12}-\sqrt{\rho_{i,j-\frac12}\rho_{i-\frac12,j}}(\delta_2v_1)_{i,j-\frac12}}{h_1h_2}+\frac{\rho_{i,j+\frac12}(\delta_2v_2)_{i,j+\frac12}-\rho_{i,j-\frac12}(\delta_2v_2)_{i,j-\frac12}}{h_2^2}\right)\Bigg]\\
&=\sum_{i,j}\Bigg[\frac{\rho_{i+\frac12,j}(w_1)_{i,j}((v_1)_{i+1,j}-(v_1)_{i,j})-\rho_{i-\frac12,j}(w_1)_{i,j}((v_1)_{i,j}-(v_1)_{i-1,j})}{h_1^2}\\
&\quad+\frac{\sqrt{\rho_{i-\frac12,j+1}\rho_{i,j+\frac12}}(w_1)_{i,j}((v_2)_{i,j+1}-(v_2)_{i-1,j+1})-\sqrt{\rho_{i-\frac12,j}\rho_{i,j-\frac12}}(w_1)_{i,j}((v_2)_{i,j}-(v_2)_{i-1,j})}{h_1h_2}\\
&\quad+\frac{\sqrt{\rho_{i+1,j-\frac12}\rho_{i+\frac12,j}}(w_2)_{i,j}((v_1)_{i+1,j}-(v_1)_{i+1,j-1})-\sqrt{\rho_{i,j-\frac12}\rho_{i-\frac12,j}}(w_2)_{i,j}((v_1)_{i,j}-(v_1)_{i,j-1})}{h_1h_2}\\
&\quad+\frac{\rho_{i,j+\frac12}(w_2)_{i,j}((v_2)_{i,j+1}-(v_2)_{i,j})-\rho_{i,j-\frac12}(w_2)_{i,j}((v_2)_{i,j}-(v_2)_{i,j-1})}{h_2^2}\Bigg]\\
&=\sum_{i,j}\Bigg[(v_1)_{i,j}\left(\frac{\rho_{i-\frac12,j}(w_1)_{i-1,j}-\rho_{i+\frac12,j}(w_1)_{i,j}-\rho_{i-\frac12,j}(w_1)_{i,j}+\rho_{i+\frac12,j}(w_1)_{i+1,j}}{h_1^2}\right)\\
&+(v_2)_{i,j}\left(\frac{\sqrt{\rho_{i-\frac12,j}\rho_{i,j-\frac12}}(w_1)_{i,j-1}-\sqrt{\rho_{i+\frac12,j}\rho_{i+1,j-\frac12}}(w_1)_{i+1,j-1}-\sqrt{\rho_{i-\frac12,j}\rho_{i,j-\frac12}}(w_1)_{i,j}+\sqrt{\rho_{i+\frac12,j}\rho_{i+1,j-\frac12}}(w_1)_{i+1,j}}{h_1h_2}\right)\\
&+(v_1)_{i,j}\left(\frac{\sqrt{\rho_{i,j-\frac12}\rho_{i-\frac12,j}}(w_2)_{i-1,j}-\sqrt{\rho_{i,j+\frac12}\rho_{i-\frac12,j+1}}(w_2)_{i-1,j+1}-\sqrt{\rho_{i,j-\frac12}\rho_{i-\frac12,j}}(w_2)_{i,j}+\sqrt{\rho_{i,j+\frac12}\rho_{i-\frac12,j+1}}(w_2)_{i,j+1}}{h_1h_2}\right)\\
&\quad+(v_2)_{i,j}\left(\frac{\rho_{i,j-\frac12}(w_2)_{i,j-1}-\rho_{i,j+\frac12}(w_2)_{i,j}-\rho_{i,j-\frac12}(w_2)_{i,j}+\rho_{i,j+\frac12}(w_2)_{i,j+1}}{h_2^2}\right)\Bigg]\\
&=\sum_{i,j}\Bigg[(v_1)_{i,j}\left(\frac{\rho_{i+\frac12,j}(\delta_1w_1)_{i+\frac12,j}-\rho_{i-\frac12,j}(\delta_1w_1)_{i-\frac12,j}}{h_1^2}+\frac{\sqrt{\rho_{i-\frac12,j+1}\rho_{i,j+\frac12}}(\delta_1w_2)_{i-\frac12,j+1}-\sqrt{\rho_{i-\frac12,j}\rho_{i,j-\frac12}}(\delta_1w_2)_{i-\frac12,j}}{h_1h_2}\right)\\
&\quad+(v_2)_{i,j}\left(\frac{\sqrt{\rho_{i+1,j-\frac12}\rho_{i+\frac12,j}}(\delta_2w_1)_{i+1,j-\frac12}-\sqrt{\rho_{i,j-\frac12}\rho_{i-\frac12,j}}(\delta_2w_1)_{i,j-\frac12}}{h_1h_2}+\frac{\rho_{i,j+\frac12}(\delta_2w_2)_{i,j+\frac12}-\rho_{i,j-\frac12}(\delta_2w_2)_{i,j-\frac12}}{h_2^2}\right)\Bigg]\\
&=\sum_{i,j}\mathrm{div}(\rho\nabla^T\mathbf{w})_{i,j}\cdot\mathbf{v}_{i,j}.
\end{aligned}
$$

References

[1] J. Ansgar. Global weak solutions to compressible Navier–Stokes equations for quantum fluids. *SIAM J. Math. Anal.*, 42(3):1025–1045, 2010.

[2] D. Bresch, N. Cellier, F. Couderc, M. Gisclon, P. Noble, G. L. Richard, C. Ruyer-Quil, and J. P. Vila. Augmented skew-symmetric system for shallow-water system with surface tension allowing large gradient of density. *J. Comput. Phys.*, 419: article no. 109670, 2020.

[3] D. Bresch, F. Couderc, P. Noble, and J. P. Vila. A generalization of the quantum Bohm identity: hyperbolic CFL condition for Euler–Korteweg equations. *Comptes Rendus. Mathématique*, 354(1):39–43, 2016.

[4] D. Bresch and B. Desjardins. Existence of global weak solutions for a 2D viscous shallow water equations and convergence to the quasi-geostrophic model. *Commun. Math. Phys.*, 238(1-2):211–223, 2003.

[5] D. Bresch and B. Desjardins. On some compressible fluid models: Korteweg, lubrication, and shallow water systems. *Commun. Partial Differ. Equations*, 28(3-4):843–868, 2003.

[6] D. Bresch, B. Desjardins, and E. Zatorska. Two-velocity hydrodynamics in fluid mechanics: Part II. Existence of global κ-entropy solutions to the compressible Navier–Stokes systems with degenerate viscosities. *J. Math. Pures Appl.*, 104(4):801–836, 2015.

[7] D. Bresch, M. Gisclon, and I. Lacroix-Violet. On Navier–Stokes–Korteweg and Euler–Korteweg systems: application to quantum fluids models. *Arch. Ration. Mech. Anal.*, 233(3):975–1025, 2019.

[8] D. Bresch, M. Gisclon, I. Lacroix-Violet, and A. Vasseur. On the exponential decay for compressible Navier–Stokes–Korteweg equations with a drag term. *J. Math. Fluid Mech.*, 24(1): article no. 11 (16 pages), 2022.

[9] S. Brull and F. Méhats. Derivation of viscous correction terms for the isothermal quantum Euler model. *Z. Angew. Math. Mech.*, 90(3):219–230, 2010.

[10] S. Busto, M. Dumbser, C. Escalante, N. Favrie, and S. Gavrilyuk. On high order ADER Discontinuous Galerkin schemes for first order hyperbolic reformulations of nonlinear dispersive systems. *J. Sci. Comput.*, 87: article no. 48, 2021.

[11] F. Dhaouadi and M. Dumbser. A first order hyperbolic reformulation of the Navier–Stokes–Korteweg system based on the GPR model and an augmented Lagrangian approach. *J. Comput. Phys.*, 470: article no. 111544, 2022.

[12] F. Dhaouadi and M. Dumbser. A Structure-Preserving Finite Volume Scheme for a Hyperbolic Reformulation of the Navier–Stokes–Korteweg Equations. *Mathematics*, 11(4): article no. 876, 2023.

[13] F. Dhaouadi, N. Favrie, and S. Gavrilyuk. Extended Lagrangian approach for the defocusing nonlinear Schrödinger equation. *Stud. Appl. Math.*, 142(3):336–358, 2019.

[14] F. Dhaouadi, S. Gavrilyuk, and J. P. Vila. Hyperbolic relaxation models for thin films down an inclined plane. *Appl. Math. Comput.*, 433: article no. 127378, 2022.

[15] D. Diehl, J. Kremser, D. Kröner, and C. Rohde. Numerical solution of Navier–Stokes–Korteweg systems by Local Discontinuous Galerkin methods in multiple space dimensions. *Appl. Math. Comput.*, 272(2):309–335, 2016.

[16] G. A. El, V. V. Geogjaev, A. V. Gurevich, and A. L. Krylov. Decay of an initial discontinuity in the defocusing NLS hydrodynamics. *Phys. D: Nonlinear Phenom.*, 87(1):186–192, 1995.

[17] G. A. El, R. H. J. Grimshaw, and N. F. Smyth. Unsteady undular bores in fully nonlinear shallow-water theory. *Phys. Fluids*, 18(2): article no. 027104, 2006.

[18] G. A. El and M. A. Hoefer. Dispersive shock waves and modulation theory. *Phys. D: Nonlinear Phenom.*, 333:11–65, 2016.

[19] C. L. Gardner. The quantum hydrodynamic model for semiconductor devices. *SIAM J. Appl. Math.*, 54(2):409–427, 1994.

[20] M. Gisclon and I. Lacroix-Violet. About the barotropic compressible quantum Navier–Stokes equations. *Nonlinear Anal., Theory Methods Appl.*, 128:106–121, 2015.

[21] H. Gomez, T. J. R. Hughes, X. Nogueira, and V. M. Calo. Isogeometric analysis of the isothermal Navier–Stokes–Korteweg equations. *Comput. Methods Appl. Mech. Eng.*, 199(25):1828–1840, 2010.

[22] A. V. Gurevich and A. P. Meshcherkin. Expanding self-similar discontinuities and shock waves in dispersive hydrodynamics. *Zh. Èksper. Teor. Fiz.*, 87:1277–1292, 1984.

[23] T. Hitz, J. Keim, C. D. Munz, and C. Rohde. A parabolic relaxation model for the Navier–Stokes–Korteweg equations. *J. Comput. Phys.*, 421: article no. 109714, 2020.

[24] A. Jüngel and P. Milišić. Full compressible Navier–Stokes equations for quantum fluids: Derivation and numerical solution. *Kinet. Relat. Models*, 4(3):785–807, 2011.

[25] A. M. Kamchatnov. *Nonlinear Periodic Waves and Their Modulations*. World Scientific, 2000.

[26] J. Keim, C. D. Munz, and C. Rohde. A relaxation model for the non-isothermal Navier–Stokes–Korteweg equations in confined domains. *J. Comput. Phys.*, 474: article no. 111830, 2023.

[27] I. Lacroix-Violet and A. Vasseur. Global weak solutions to the compressible quantum Navier–Stokes equation and its semi-classical limit. *J. Math. Pures Appl.*, 114:191–210, 2018.

[28] E. Madelung. Quantentheorie in hydrodynamischer Form. *Z. Phys.*, 40:322–326, 1927.

[29] A. Martínez, L. Ramírez, X. Nogueira, S. Khelladi, and F. Navarrina. A high-order finite volume method with improved isotherms reconstruction for the computation of multiphase flows using the Navier–Stokes–Korteweg equations. *Comput. Math. Appl.*, 79(3):673–696, 2020.

[30] J. Neusser, C. Rohde, and V. Schleper. Relaxation of the Navier–Stokes–Korteweg equations for compressible two-phase flow with phase transition. *Int. J. Numer. Methods Fluids*, 79(12):615–639, 2015.

[31] C. Ruyer-Quil, D. Bresch, M. Gisclon, G. L. Richard, M. Kessar, and N. Cellier. Sliding and merging of strongly sheared droplets. *J. Fluid Mech.*, 972: article no. A40, 2023.

[32] L. Tian, Y. Xu, J. G. M. Kuerten, and J. J. W. Van der Vegt. A local Discontinuous Galerkin method for the (non)-isothermal Navier–Stokes–Korteweg equations. *J. Comput. Phys.*, 295:685–714, 2015.

[33] G. B. Whitham. *Linear and Nonlinear Waves*. John Wiley & Sons, 2011.